

Research Paper

Reliability analysis of 1D estimation for TBM operational parameters

Oveis Farzay*, Marilena Cardu

Environment, Land and Infrastructure Engineering Department, Politecnico di Torino, Torino 10129, Italy

Received 21 May 2025; received in revised form 4 September 2025; accepted 28 October 2025

Available online 5 January 2026

Abstract

Accurate TBM performance estimation is essential for effective tunnel design and planning. This study introduces a one-dimensional (1D) estimation model that estimates thrust, torque, power, cutterhead speed, and tool count using only excavation diameter. The model was developed across four TBM types—open, single shield (SS), double shield (DS), and earth pressure balance (EPB)—to isolate the influence of diameter from other variables. Validation against existing models and a 52-case independent dataset confirmed strong correlations: torque scales with the cube of the excavation diameter ($R^2 = 0.89$ for EPB), power grows faster than linearly ($R^2 = 0.83$ for EPB), thrust increases supra-linearly ($R^2 = 0.79$ for EPB), and cutterhead speed decreases with diameter ($R^2 = 0.87$ for open TBM). Tool count grows proportionally. A reliability matrix compares model accuracy and data support, aiding selection based on both fitness and robustness. This 1D model offers fast, consistent estimates for early-stage assessments. While it excludes detailed geological input, it is suited for feasibility studies and preliminary design. Future work will incorporate additional ground and machine parameters and extend validation across a broader range of tunneling conditions to enhance generalizability.

Keywords: 1D model; Excavation diameter; TBM operational parameters; Reliability matrix

1 Introduction

Since James Robbins introduced the first modern TBM for the Oahe Dam Project in South Dakota in 1952, reliable models for predicting TBM design and performance have emerged as a central concern (Sutcliffe, 1996). When conducting metal wear analyses (Cardu et al., 2023a), forecasting penetration rates and advance rates during rock excavation (Cardu et al., 2024), or determining the face support pressure for earth pressure balance (EPB) machines (Zhai et al., 2024), predictive models empower engineers to estimate project timelines, costs, and challenges, ensuring efficient resource allocation.

Several TBM performance prediction models, broadly classified into four categories, have been developed to address this need. The first consists of empirical models based on field observations (Graham, 1976). Although

these models are easy to use, their predictive accuracy is often limited because they consider only a narrow range of parameters. Additional empirical models have combined the field penetration index with rock mass classification methods such as the RMR, the Q-system, and GSI, enhancing TBM performance prediction in complex geological environments (Hassanpour et al., 2011).

For EPB machines operating in soft and mixed ground, empirical methods have incorporated factors such as the main drive torque, initially through simple coefficients (Krause, 1987) and later through comprehensive torque models that account systematically for friction, cutting forces, and shearing resistance (Wang et al., 2012). Further studies have refined earth pressure support models to enhance facial stability prediction and operational safety (Song & Zhou, 2008).

The second category includes multiple parameter models, such as the Colorado School of Mines (CSM) model (Rostami, 1997; Rostami & Ozdemir, 1993), the Norwegian University of Science and Technology (NTNU) model (Bruland, 1998), and the Q-system-based TBM model

* Corresponding author.

E-mail address: oveis.farzay@polito.it (O. Farzay).
Peer review under the responsibility of Tongji University

(Barton, 1999). The CSM model relies primarily on intact rock properties, such as uniaxial compressive strength, Brazilian tensile strength, and the Cerchar abrasivity index (Cardu et al., 2023b; Farzay et al., 2022a, 2022b; Khatibi et al., 2018a, 2018b, 2019; Shakouri et al., 2019), but it does not sufficiently account for jointed and fractured rock masses (Farrokh et al., 2012). Efforts to improve its predictive ability have included incorporating additional rock mass parameters (Yagiz, 2002) and applying adjustment factors for complex conditions (Ramezanzadeh et al., 2005). In contrast, the NTNU model integrates geological and operational parameters, with recent updates such as the rolling indentation abrasion test, enhancing cutter wear predictions (Macias, 2016).

The third category, probabilistic models, accounts for the inherent variability in TBM performance (Laughton, 1998). However, their practical applicability is often limited by their reliance on incomplete datasets, site-specific variability, and dependence on expert judgment rather than comprehensive data (Jodehl et al., 2025; Mostafa & Sousa, 2024).

The fourth category includes computer-aided models, which utilize extensive databases to improve prediction accuracy. However, these models are typically complex and not publicly accessible (Farzay et al., 2025; Grima & Babuška, 1999). Parallel advancements in EPB machine control systems have contributed to operational efficiency.

All the performance prediction categories discussed above are mostly based on the use of geology as an input to perform the prediction, which is necessary since geological conditions impact TBM performance. Figure 1 shows the effect of geology on the TBM performance parameters for each TBM type (the values shown are for relative comparison only and are not derived from quantitative calibration).

Geology strongly influences TBM performance, especially in EPB and single-shield (SS) types, where parameters such as thrust, torque, power, and tool wear are highly affected. EPBs are sensitive to soil cohesion, perme-

ability, and conditioning, while SS TBMs respond to rock strength, fracturing, and abrasivity (Bilgin & Acun, 2021; Samadi & Hassanpour, 2024). Double shield (DS) TBMs show moderate-to-strong geological influence, particularly on thrust and cutter wear in transitional rock. Open TBMs are less sensitive but still affected by abrasive or hard rock. These findings confirm that geology is a key input in performance prediction models for all TBM types (Cardu et al., 2021; Pandey et al., 2020).

Diameter selection must balance geology, method, cost, function, and safety. Use determines internal dimensions (Lu et al., 2023), and proper sizing improves TBM design and function (Vardakos et al., 2023). Though the function defines the initial diameter, geology, logistics, and safety may require changes (Qian et al., 2019). Diameters may change mid-project. For instance, Mill Creek's tunnel shrank from 11.6 to 9.9 m due to ground conditions (Caulfield et al., 2005), while Claremont and Eurasia tunnels grew to meet seismic standards (Tunneling and Underground Construction, 2023).

Several studies explored how changes in diameter affect thrust, torque, power, and wear. Howart (1994), emphasized geology's role. Ates et al. (2014), Cardu et al. (2021), and Park et al. (2018) extended this to more parameters across TBM types and geologies. However, limitations remain. Park's data cover only the 6–10 m range, Ates lacks large-diameter machines, installed power is underrepresented, and none of these models incorporate independent validation or structured reliability checks. The reliance on small, outdated datasets with limited comparisons further reduces real-world applicability.

This study analyzes 302 TBMs across all major types. For each type, statistical fits were applied between diameter and thrust, torque, power, cutterhead speed (RPM), and tool count, with best-fit equations compared to the models of Park, Ates, and Howarth (DE = this study's equations). A validation dataset was used to test performance, yielding sixteen top models. Beyond extending coverage, this study also addresses the broader issue of how reliable 1D diameter-based modeling can be, to what extent engineers can rely on such predictions, under which conditions these models are useful for feasibility and preliminary design, and when geological or other factors must take precedence.

2 Overview of the database

It is important to carefully review each dataset used in this study to understand the reliability and accuracy of the equations. This paper utilizes a database comprising specifications of 302 TBMs manufactured after 1985 (Bilgin et al., 1999, 2012; Cardu et al., 2021, 2023a, 2024; Chang et al., 2006; Chapis & Yiu, 2006; Cho et al., 2013; Garshol et al., 2000; Hassanpour et al., 2015; Keiper et al., 2010; Moon & Oh, 2012; Okano et al., 2000; Ozdemir, 1977; Partov et al., 2012; Pompeu-Santos, 2011; Qi et al., 2016; Rostami, 2016; Rostami et al., 2014; Rostami & Ozdemir, 1993; Salimi et al., 2018,

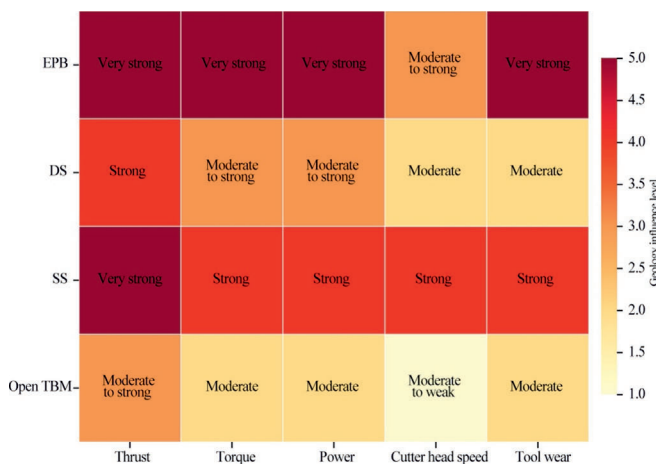


Fig. 1. Geological influence on the TBM performance parameters.

2019; Sun et al., 2018; Wilfing, 2016; Zheng & He, 2021; Yazdani-Chamzini & Yakhchali, 2012; Zhang et al., 2013, 2012). The dataset provides the empirical foundation for the analyses in the following sections, encompassing a diverse range of TBM types, geographical settings, and operational conditions. This diversity enables a robust evaluation of model performance across various excavation scenarios.

Figure 2 shows the distribution of TBM type in the dataset. Open TBMs make up 34.8% (105 entries), followed by DS at 32% (97), EPB at 16.6% (50), and SS at 11.6% (36). Multimode TBMs (5.0%, 15 entries) were excluded due to inconsistent classification. Rock parameters like UCS and RMR often lack sufficient coverage to support strong correlations. Although lithological data are commonly reported, they are typically too general to build reliable models for specific rock types.

The dataset spans global TBM projects, with major clusters in East Asia, Europe, and North America, capturing diverse geology and construction practices.

Figure 3 presents the frequency distribution of key parameters derived from the compiled dataset to assess the scope and variability of the operational inputs.

- Figure 3(a) – Excavation diameter (m): Excavation diameters range from approximately 2 to 14 m, with the most frequent interval falling between 4 and 6 m.
- Figure 3(b) – Power (kW): Installed TBM power shows a strong concentration between 1000 and 3000 kW. The limited number of entries exceeded 5000 kW.
- Figure 3(c) – Thrust (kN): Thrust values are below 25 000 kN, although a few extreme cases surpass 150 000 kN.

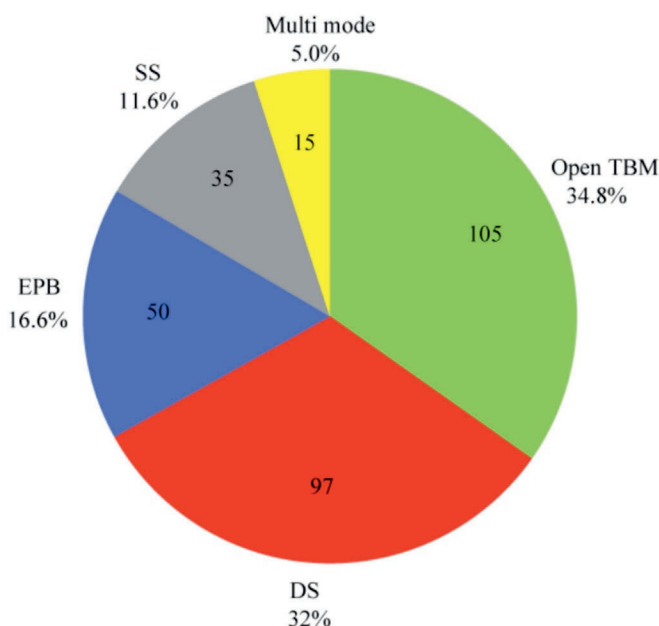


Fig. 2. TBM types according to the dataset.

- Figure 3(d) – Torque (kN·m): Torque values are mostly less than 10 000 kN·m. Entries exceeding 30 000 kN·m can be considered high.
- Figure 3(e) – Cutterhead speed (RPM, r/min): Cutterhead speeds vary broadly between 2 and 16 r/min.

The Park dataset includes specs and performance data for 270 TBMs built after 2000. Most (71.1%) are medium-diameter (6–10 m), followed by large (10–14 m, 23%) and ultra-large (>14 m, 5.9%). EPBs dominate (53.7%), followed by slurry (21.5%), DS (7.8%), open TBM (6.3%), SS (5.9%), and multimode (4.8%). Slurry and multimode TBMs (26.3%) were excluded from this study. The Ates dataset contains 262 TBMs manufactured after 1985, with 86 EPBs (32.8%), 72 open TBMs (27.5%), 41 DS (15.6%), 39 slurry (14.9%), and 24 SS (9.2%). Most have diameters above 4 m; smaller units are rare.

The validation dataset includes 52 TBMs and was developed to independently test the predictive accuracy of regression models from the Park, Ates, and the current study datasets. (Ates et al., 2014; Ban et al., 2020; Bbt, 2025; Brenner Basistunnel, 2025; Co, 2025; Herrenknecht, 2024, 2025a, 2025b, 2025c; Implenia, 2023; King et al., 2017; Merguerian, 2010; Staff, 2024, 2000; The Robbins, 2025; Thibault, 2024; Thomas, 2024; Tunnel, 2025; Wikipedia, 2025; Yagiz & Ozdemir, 2001). This dataset was excluded from model development to ensure objective validation and prevent overfitting. EPBs are the most common type (37.5%). Diameters range from 3.0 to 14.4 m, covering both small and large TBMs. Table 1 shows the contribution of the TBM type to each dataset.

New models (DEs) are compared with those by Park and Ates. Four metrics are used: R^2 (explained variance), root mean square error (RMSE), Akaike information criterion (AIC), and Bayesian information criterion (BIC), which penalize model complexity. RMSE is also expressed as a percentage of the maximum observed value to support practical interpretation. Cross-validated RMSE is calculated via repeated subsampling to evaluate performance on unseen data.

Model validation is performed in two steps: relative analysis and absolute analysis. In the relative analysis, all candidate models within each TBM type (Open, SS, DS, EPB) are compared using R^2 , RMSE, AIC, and BIC for a given TBM type, and the model that combines the highest R^2 with the lowest AIC, BIC, and RMSE is regarded as the best performing model in that group. This step, therefore, provides a ranking of competing models and identifies a single leading model for each TBM type.

Once the leading model has been identified for each TBM type, an absolute analysis is used to evaluate its practical reliability. In this step, RMSE is expressed as a percentage of the maximum observed value of the target variable, and a cross-validated RMSE is obtained by repeated subsampling to approximate performance on unseen data. A model is considered robust when it leads its group in the relative analysis, its RMSE percentage is

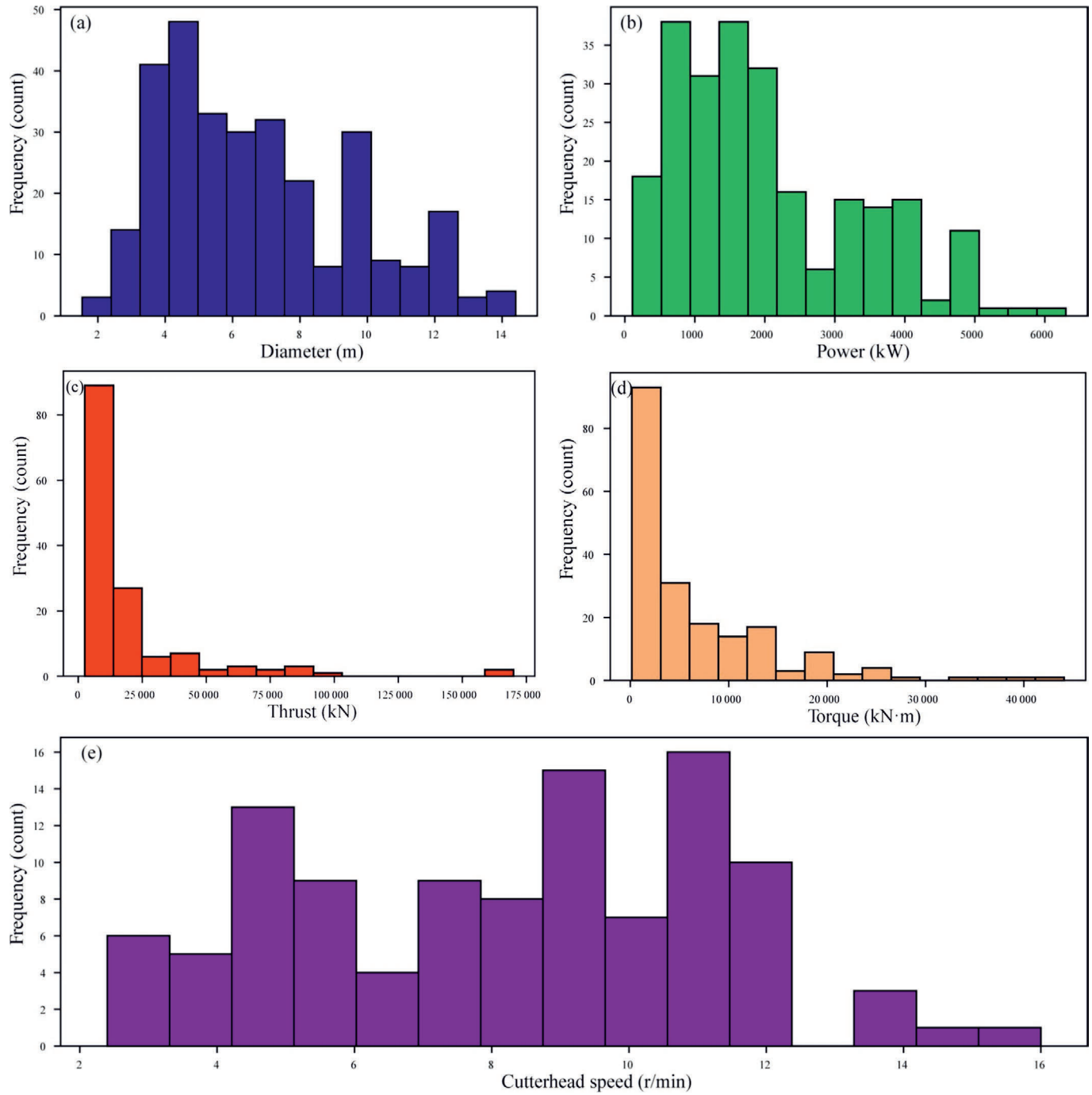


Fig. 3. Histograms of the distributions of critical operational parameters of TBMs in the database. (a) Diameter, (b) power, (c) thrust, (d) torque, and (e) cutterhead speed.

Table 1
 Details of each TBM type in the Park, Ates, current study, and validation datasets.

Dataset	Total cases	Open TBM (%)	DS (%)	EPB (%)	SS (%)	Multimode + Slurry (%)
Park	270	6.3	7.8	53.7	5.9	26.3
Ates	262	27.5	15.6	32.8	9.2	14.9
Current study	302	34.8	32	16.6	11.6	5
Validation	52	17.3	21.2	38.5	23	0

small compared to the range of observed values, and the increase in RMSE under cross-validation is limited. Under this framework, reporting RMSE as a percentage and evaluating the change in RMSE under cross validation constitutes the absolute analysis and indicates whether the selected model is suitable for real-world prediction.

3 TBM operational parameters

The main operational parameters of a TBM are critical to its performance during tunneling and are summarized below.

3.1 Thrust

TBM thrust arises from multiple components. Shield-ground friction, often dominant in clayey or abrasive soils,

depends on geological conditions and lubrication effectiveness. In pressurized TBMs, the facial pressure resists earth and water forces. Curved alignments require additional thrust for steering, while straight tunnels require less. Tail seal friction occurs as lining segments pass through seals and must be overcome with a steady force to prevent damage. Thrust is also required to advance the trailing backup unless it's self-propelled. In hard ground with Open TBMs, penetration force becomes critical as cutters engage rock, but this contribution is minimal in soft soils.

Thrust increases with TBM diameter (see Figs. 4 and 5), due to a larger shield-ground contact area and a larger face area. Both shield friction and face resistance scale approximately with the square of diameter. In squeezing ground, thrust may double, and changes in friction coefficients can alter thrust by up to 300%. Larger diameters, therefore, amplify geometric and ground interaction forces, making

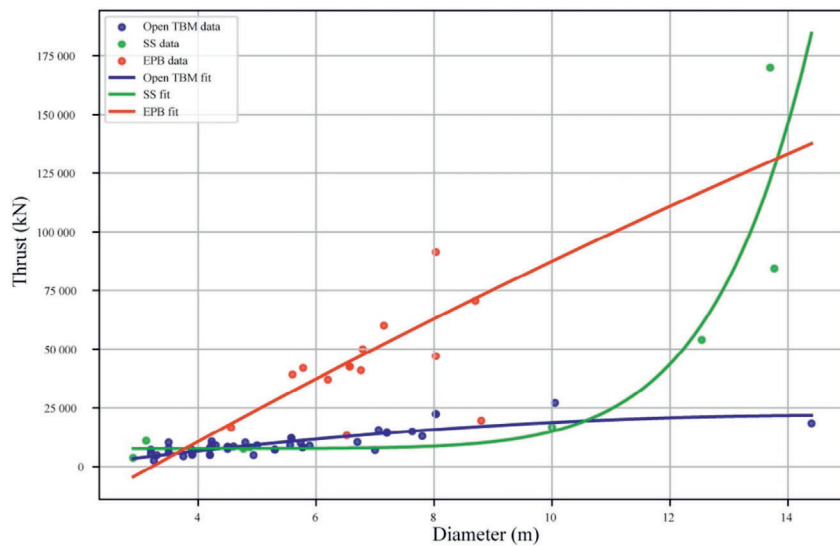


Fig. 4. Thrust vs. diameter for Open TBM, EPB, and SS.

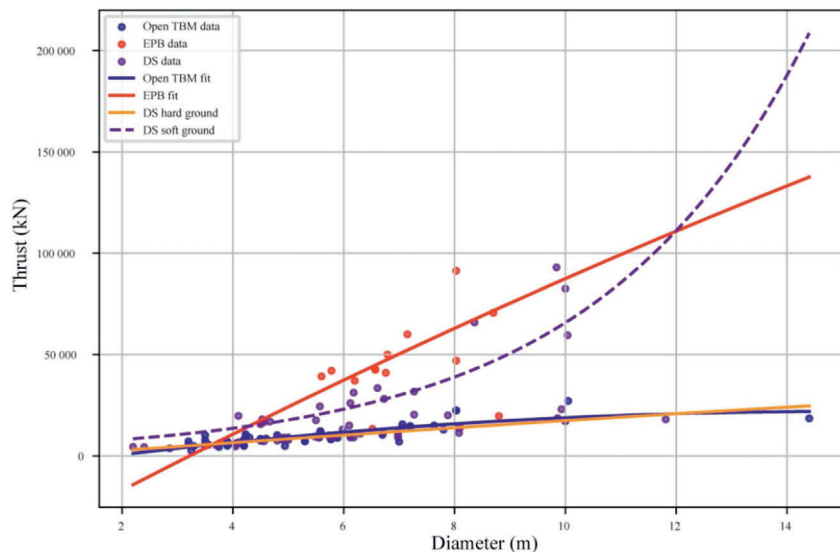


Fig. 5. Thrust vs. diameter for Open TBM, EPB, and DS.

diameter a key factor in thrust design (Machida & Uomoto, 1997).

EPBs generally require higher thrust, reflecting the contributions of all components. In contrast, Open TBMs mainly rely on penetration force and, occasionally, backup drag. Figure 4 shows that EPBs consistently exhibit higher thrust values than Open and SS TBMs at the same diameter.

Open TBMs show a moderate, nearly linear thrust increase with diameter, driven mainly by cutter penetration and minimal backup drag. EPBs follow a much steeper trend, reflecting the rising effects of face pressure and shield–soil friction with diameter. SS TBMs display distinct behavior: up to ~10 m, their thrust resembles that of Open TBMs, as both operate in rock with minimal friction and no chamber pressure. Beyond this threshold, SS thrust rises sharply and nonlinearly, likely due to increased resistance in fractured ground, which complicates advancement.

Figure 5 presents thrust as a function of TBM diameter for Open, EPB, and DS machines. It includes observed data and fitted curves, with DS values split into two categories, hard and soft ground, based on behavioral trends. Since geological records are incomplete, this classification is empirical: DS curves resembling EPBs are labeled “soft ground”, while those aligning with Open TBMs are labeled “hard ground”. This separation allows clearer interpretation of DS thrust responses across different operating conditions.

The behavior of DS TBMs follows a more complex pattern, with two distinct fit lines corresponding to different geological conditions. The yellow line represents DS TBMs operating in hard rock environments, with a trend closely aligned with that of single-shield and open TBMs. This suggests that thrust is governed primarily by mechanical penetration and limited frictional forces in such settings, as previously observed in rock-dominated conditions. In contrast, the dashed purple line illustrates the behavior of DS TBMs in soft ground, where the thrust requirement escalates sharply with increasing diameter. This indicates that weak or deformable ground conditions introduce additional resistance factors, such as shield–soil interactions, segment–seal friction, and face instability, all of which significantly contribute to the overall thrust demand.

Table 2 presents a comprehensive collection of equations that relate the required thrust force F_N to the TBM diameter across different machine types and geological settings. Each entry includes the geological condition under which the equation was derived, the form of the equation itself, the coefficient of determination (R^2) indicating the model’s fit to its dataset, and the source.

The validation dataset was used to evaluate the absolute and relative accuracy of all thrust–diameter equations in Table 2. Figure 6 shows model predictions versus observed values, grouped by TBM type, highlighting alignment quality.

For open TBMs (Fig. 6(a)), the DE model is most reliable, with $R^2 = 0.55$, RMSE = 4 MN, and the lowest AIC (20.6) and BIC (20.2). The RMSE corresponds to 2.22% of the maximum thrust, and cross-validation increases it by only 0.23%, confirming stable performance. For SS TBMs (Fig. 6(b)), the Ates model is identified as the best, explaining 42% of thrust variability ($R^2 = 0.42$) and producing the lowest RMSE (21.42 MN), AIC (77.5), and BIC (78.5). RMSE decreases from 11.9% to 11.35% under cross-validation, indicating good generalizability. For DS TBMs (Fig. 6(c)), the DE Soft Ground model performs best, with $R^2 = 0.68$, RMSE = 13.69 MN, and the lowest AIC (56.3) and BIC (56.9). RMSE drops from 7.6% to 7.14% in cross-validation, reflecting accurate and stable performance. For EPBs (Fig. 6(d)), the Ates model is preferred, achieving $R^2 = 0.79$, RMSE = 18.82 MN, and the lowest AIC (74.4) and BIC (75.4). RMSE decreases from 10.5% (18,815 kN) to 9.8% (17,719 kN) under cross-validation, confirming strong generalization.

3.2 Torque

Cutterhead torque generally increases with the cube of TBM diameter, following geometric scaling laws (Machida & Uomoto, 1997). Shi et al. (2011) defined total torque as the sum of eight components: frontal (T_1), side (T_2), and back surface friction (T_3); tool cutting resistance (T_4); shear at openings (T_5); muck mixing in EPB chambers (T_6); main bearing resistance (T_7); and seal friction (T_8). These depend

Table 2
Summary of thrust estimation equations $F_N(D)$ for different TBM types under various geological conditions.

TBM type	Geological condition	Equation $F_N(D)$	R^2	Source
DS	Fractured rock	$F_N = 6435.1D - 200.32$	0.63	Ates
DS	Squeezing ground	$F_N = 422.6D^{2.2254}$	0.79	Ates
EPB	Soft/Mixed ground	$F_N = 8972.6e^{(0.2208D)}$	0.79	Ates
Open TBM	Rock	$F_N = 1777.1D + 377.7$	0.4	Ates
SS	Fractured rock	$F_N = 1459.8D^{1.4156}$	0.42	Ates
DS	Hard ground	$F_N = -17.65D^2 + 2061.1D - 1413.5$	0.79	DE
DS	Soft ground	$F_N = 4762.2e^{(0.2625D)}$	0.61	DE
EPB	Soft/Mixed ground	$F_N = -193.77((D - 6.861)/1.201)^2 + 15411((D - 6.861)/1.201) + 48514$	0.68	DE
Open TBM	Rock	$F_N = -127.40D^2 + 3804.2D - 6497.1$	0.67	DE
SS	Fractured rock	$F_N = 1.3263 \times 10^{-5}D^{8.7411} + 7675$	0.82	DE
DS	Rock	$F_N = -150642.13 + 22659.77D$	0.8	Park
EPB	Soft ground	$F_N = e^{(10.16 + 0.02D + 0.010D^2)}$	0.83	Park
EPB	Mixed ground	$F_N = e^{(9.31 + 0.02D + 0.010D^2)}$	0.92	Park

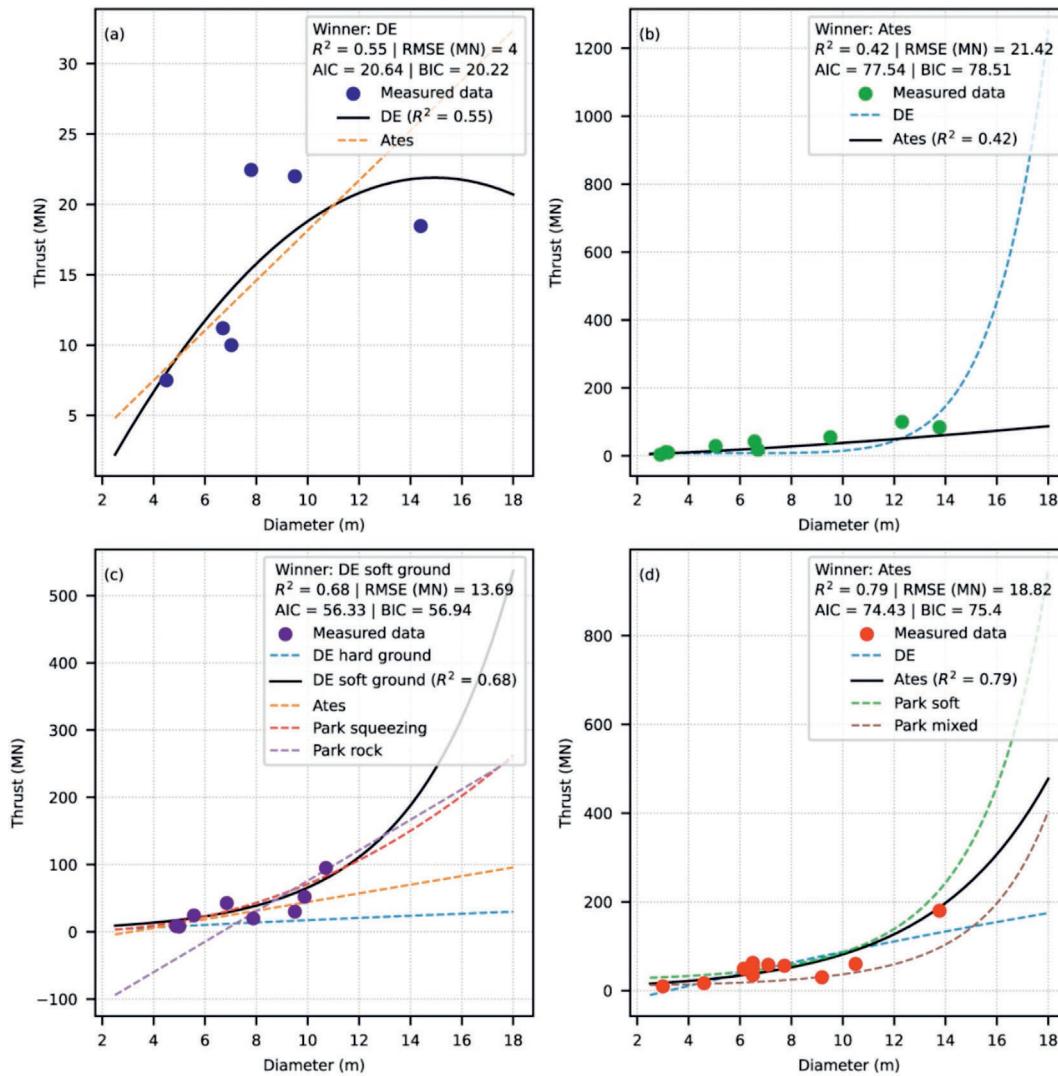


Fig. 6. Thrust versus diameter: comparison of model predictions and validation dataset results by TBM type. (a) Open TBMs, (b) SS TBMs, (c) DS TBMs, and (d) EPBs.

on factors like overburden, soil properties, cutterhead design, and machine configuration (Song et al., 2010).

At a fixed diameter, EPBs require the highest torque. According to Shi et al. (2011), T_1 – T_3 and T_6 account for up to 89% of total resistance due to mixing, pressurization, and sticky soil handling. Double-shield TBMs also exhibit high torque, driven by hard rock cutting and shield friction, especially in squeezing zones. Single shields follow, with torque affected by cutterhead–ground interaction and jamming in fractured rock. Open TBMs require the least torque, mainly from cutting (T_4), making their behavior more predictable at constant diameter. Figure 7 illustrates the torque–diameter relationship for each TBM type based on the dataset analyzed in this study.

Figure 7 confirms the torque hierarchy across TBM types. EPBs show the steepest torque increase with diameter due to internal resistance from mixing and pressurization. SS and DS TBMs display wider scatter, reflecting geological variability in fractured or squeezing ground.

Open TBMs remain the most consistent, showing the lowest torque trend and minimal deviation—typical of operation in competent rock.

The relationship between torque and diameter was modeled across TBM types by using various datasets and geological settings. Empirical equations from this study (DE) and prior work by Ates and Park are compiled in Table 3. In each equation, cutterhead torque (T , kN·m) is related to excavation diameter (D , m) under specific ground conditions, and the model form, R^2 , geological context, and data source are summarized for each case.

The validation dataset was used to evaluate the absolute and relative accuracy of all the torque–diameter equations in Table 3. Figure 8 compares the predicted and observed torque values for each TBM type, illustrating how accurately each model reflects real-world data across machine categories.

For Open TBMs (Fig. 8(a)), the Park model is most reliable, explaining 73% of thrust variability ($R^2 = 0.73$) with a

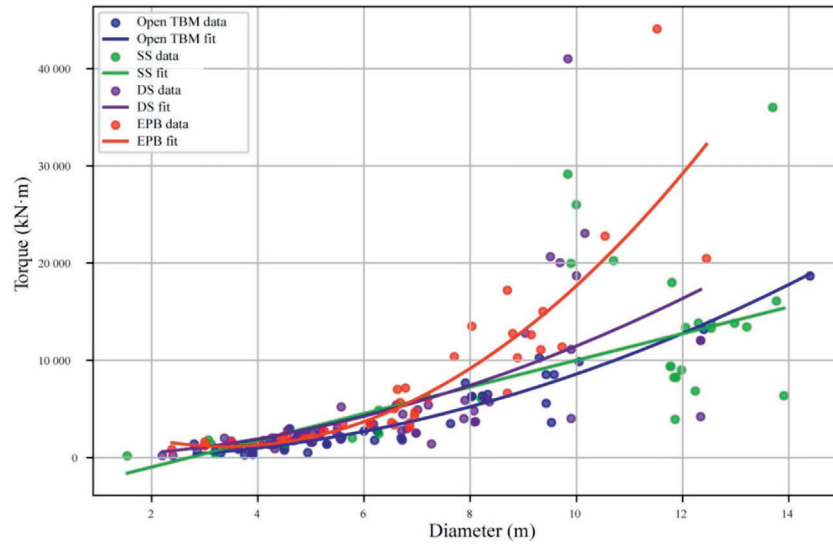


Fig. 7. Torque vs. excavation diameter for all the TBM types.

Table 3
Summary of torque estimation equations $T(D)$ for different TBM types under various geological conditions.

TBM type	Geological condition	Equation $T(D)$	R^2	Source
DS	Fractured rock	$T = 38.12D^{2.3546}$	0.79	Ates
DS	Squeezing ground	$T = 260.27D^{0.4504}$	0.98	Ates
EPB	Soft or mixed ground	$T = 13.438D^{3.154}$	0.85	Ates
Open TBM	Rock	$T = 1089.3D - 4188.8$	0.63	Ates
SS	Fractured rock	$T = 187.7D^{1.4390}$	0.66	Ates
DS	Fractured rock	$T = 129.28D^{1.948}$	0.40	DE
EPB	Soft or mixed ground	$T = 379.53D^2 - 2581.1D + 5516.7$	0.76	DE
Open TBM	Rock	$T = 103.55D^2 - 184.25D + 67.48$	0.91	DE
SS	Fractured rock	$T = 1371.9D - 3720.9$	0.46	DE
DS	Fractured rock	$T = -15\,520.13 + 3112.77D$	0.36	Park
EPB	Soft ground	$T = e^{(0.02 + 0.20D)}$	0.84	Park
EPB	Mixed ground	$T = -15\,520.13 + 3112.77D$	0.59	Park
Open TBM	Rock	$T = -8748.52 + 1834.63D$	0.82	Park

low RMSE of 9.28%. It also yields the lowest AIC and BIC values, indicating strong accuracy with minimal complexity. Cross-validation (CV RMSE = 6.74%) further confirms its stability. For SS TBMs (Fig. 8(b)), the DE model performs best, capturing 59% of thrust variation ($R^2 = 0.59$) and yielding an RMSE of 16.57%. Its AIC and BIC are lower than those of the Ates model, and cross-validation (CV RMSE = 12.99%) confirms good generalizability without signs of overfitting. For DS TBMs (Fig. 8(c)), the Park model leads again, explaining 67% of the variation ($R^2 = 0.67$) and achieving the lowest RMSE (14.21%), AIC, and BIC. Cross-validation (CV RMSE = 13.26%) shows consistent performance. For EPBs (Fig. 8(d)), the DE model is dominant, explaining 89% of thrust variation ($R^2 = 0.89$) with the lowest RMSE (8.56%) and the best AIC and BIC values. Cross-validation (CV RMSE = 7.32%) confirms its accuracy and robustness.

3.3 Cutterhead speed

A clear inverse relationship exists between TBM diameter (D) and maximum cutterhead speed (RPM): as diameter increases, cutterhead speed decreases. Larger cutterheads are heavier and face greater resistance, making fast rotation more difficult and less safe. Mechanical limits and the torque required to rotate the head also constrain the cutterhead speed (Barla & Pelizza, 2000).

For a given diameter, DS TBMs typically reach the highest cutterhead speed due to designs suited for fractured rock and faster advancement. Open TBMs also operate at high cutterhead speeds in competent rock to optimize cutting and minimize tool wear. SS TBMs run slightly slower than DS and Open types, mainly due to higher shield friction and the need for precision in fractured ground.

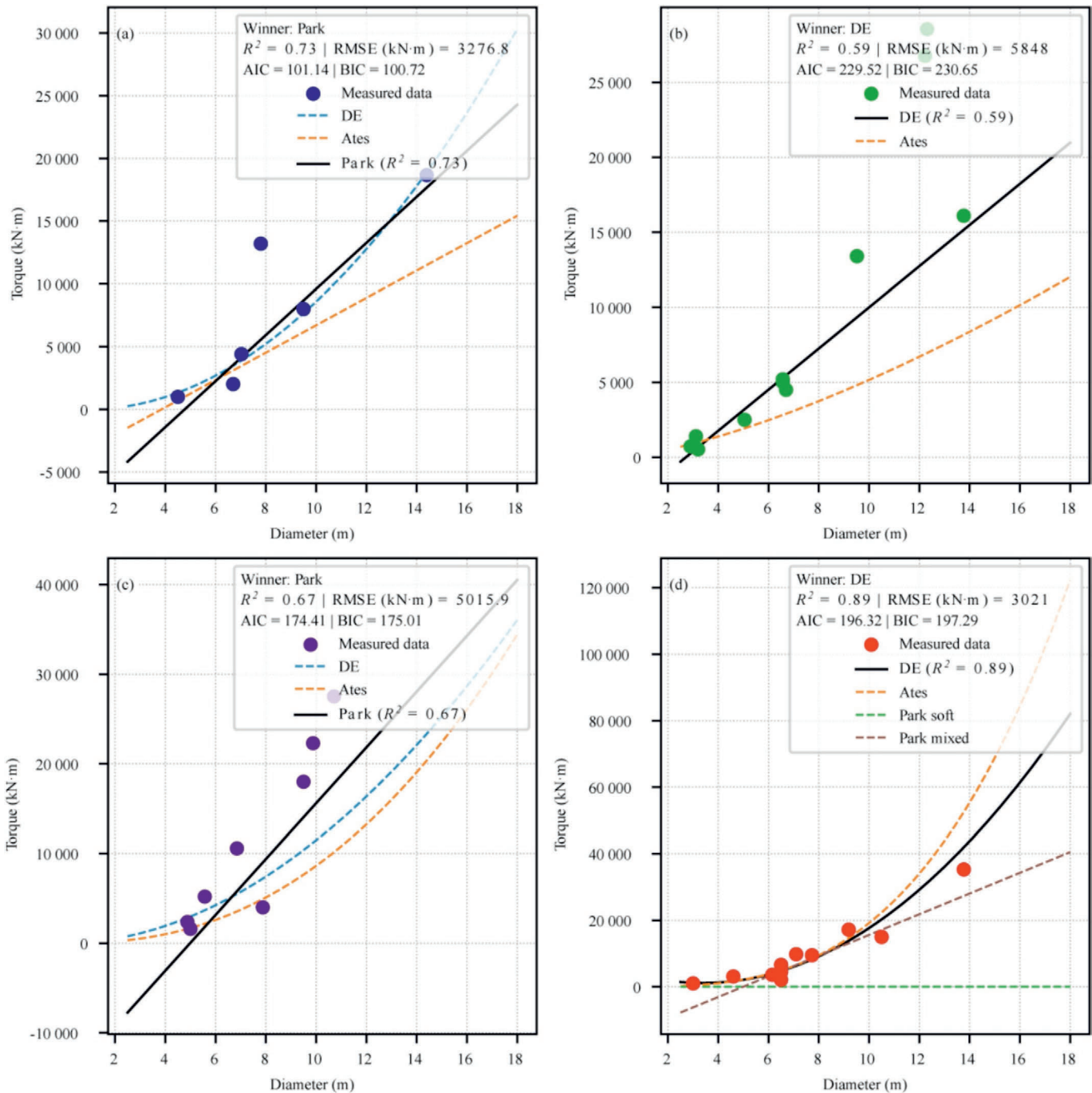


Fig. 8. Torque versus diameter: comparison of model predictions and validation dataset results by TBM type. (a) Open TBMs, (b) SS TBMs, (c) DS TBMs, and (d) EPBs.

EPBs consistently operate at the lowest cutterhead speed (typically 1–4) regardless of diameter. Their performance is highly sensitive to soil conditions, requiring strict control of face pressure and muck flow to prevent blockage and maintain stability (Bilgin & Algan, 2012; Ramoni & Anagnostou, 2010). Figure 9 illustrates how cutterhead speed varies with diameter by TBM type using this study's dataset.

Table 4 summarizes the cutterhead speed (n_{RPM})–diameter equations for different TBM types under various ground conditions. For each case, the table includes the kind of geology, the form of the model, the R^2 value, and the source.

The validation dataset was used to check the absolute and relative accuracy of all the cutterhead speed–diameter equations listed in Table 4. Figure 10 compares the predicted torque values with the actual measurements for each TBM type. This comparison shows how well each model matches real data across the different types of machines.

The Ates model performs best for the Open TBM data (Fig. 10(a)), with $R^2 = 0.87$, explaining 87% of the variation. It also has the lowest AIC (0.7) and BIC (−0.6), indicating a simple and well-fitting model. The RMSE is only 0.66 r/min (5.5%), suggesting high accuracy. Although cross-validation

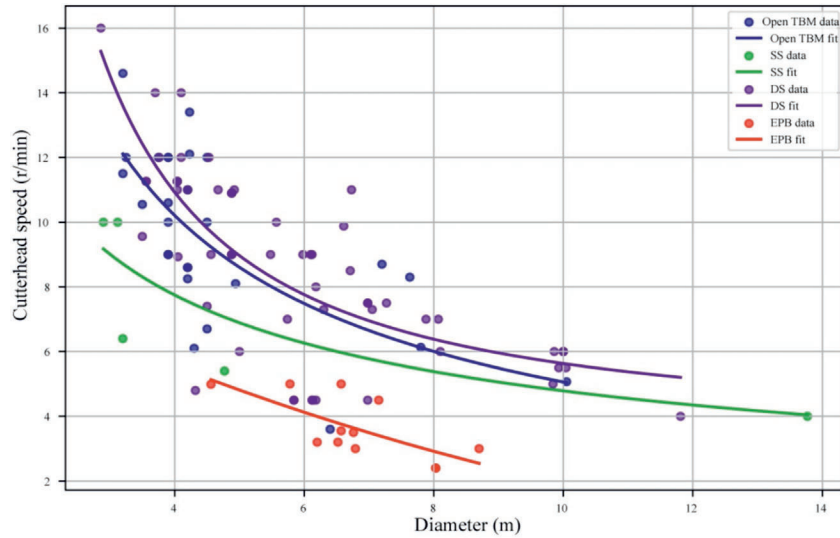


Fig. 9. Cutterhead rotational speed vs. excavation diameter for all TBM types.

Table 4

Summary of the cutterhead speed equations $n_{RPM}(D)$ for different TBM types under various geological conditions.

TBM type	Ground type	Equation $n_{RPM}(D)$	R^2	Source
Open TBM	Rock	$n_{RPM} = 28.010D^{-0.6641}$	0.88	Ates
SS	Fractured rock	$n_{RPM} = -0.629D + 11.409$	0.66	Ates
DS	Fractured rock	$n_{RPM} = 39.776D^{-0.8763}$	0.37	Ates
EPB	Soft/Mixed ground	$n_{RPM} = -0.180D + 4.846$	0.17	Ates
Open TBM	Rock	$n_{RPM} = 29.5063D^{-0.7657}$	0.46	DE
SS	Fractured rock	$n_{RPM} = 16.0559D^{-0.5257}$	0.56	DE
DS	Fractured rock	$n_{RPM} = 50.3124D^{-0.13869} + 3.5661$	0.58	DE
EPB	Soft/Mixed ground	$n_{RPM} = 0.0276D^2 - 0.9906D + 9.0756$	0.48	DE
Open TBM	Rock	$n_{RPM} = -4.389\ln(D) + 13.182$	0.27	Howart
EPB	Soft ground	$n_{RPM} = 405.44e^{-0.128D} + 2.65$	0.20	Park
EPB	Mixed ground	$n_{RPM} = 1.31e^{-0.144D} + 2.76$	0.24	Park
Open TBM	Rock	$n_{RPM} = 10.34 - 0.44D$	0.30	Park

was not possible due to limited data, the low error rate indicates good generalizability. For the SS data (Fig. 10(b)), the DE model is the most reliable, with $R^2 = 0.79$. Its AIC (8.9) and BIC (9.9) values are lower than those of the Ates model (AIC(10.9) and BIC(10.9)), indicating a better fit. The RMSE is 1.23 r/min (10.2%), which decreases to 1.11 r/min (9.3%) under cross-validation, confirming the absence of overfitting and demonstrating strong generalization capability.

The Ates model also performs well for DS data (Fig. 10(c)), explaining 49% of the variation ($R^2 = 0.49$). Its AIC (12) and BIC (12.6) values are lower than those of the DE model. The RMSE is 1.50 r/min (12.5%), improving to 1.27 r/min (10.6%) with cross-validation. For the EPB data (Fig. 10(d)), the Ates model again performs best, despite a low R^2 of 0.14. It achieves the lowest AIC (16.7) and BIC (17.7). The RMSE is 1.7 r/min (14.1%), dropping slightly to 1.63 r/min (13.6%) under cross-validation.

3.4 Power

As the tunnel diameter increases, the TBM cutterhead must deliver more energy to excavate the larger face,

despite slower rotation. The longer lever arm increases torque rapidly, while RPM drops slightly to prevent overload. As a result, installed power grows faster than diameter, making size the key driver of motor capacity. On-site teams adjust this power based on ground conditions (e.g., rock strength, jointing, soil type) to maintain steady progress without excess energy use.

EPBs generally have the highest installed power at a given diameter, followed by double-shield, single-shield, and open TBMs. EPBs require more energy for soil conditioning, face pressure, and muck handling. Shielded machines experience additional friction and require more complex control systems. Although machines can be ranked by typical power, actual power demand depends on geology, additives, advance rate, and operational strategy, and often varies by 20%–50%. Figure 11 shows the correlation between excavation diameter and power; consumed power cannot be ordered strictly by TBM type.

TBM power ratings increase sharply with diameter, but the rate and variability depend on machine type and ground conditions. Open and double-shield TBMs show near-linear trends, while single-shield machines increase

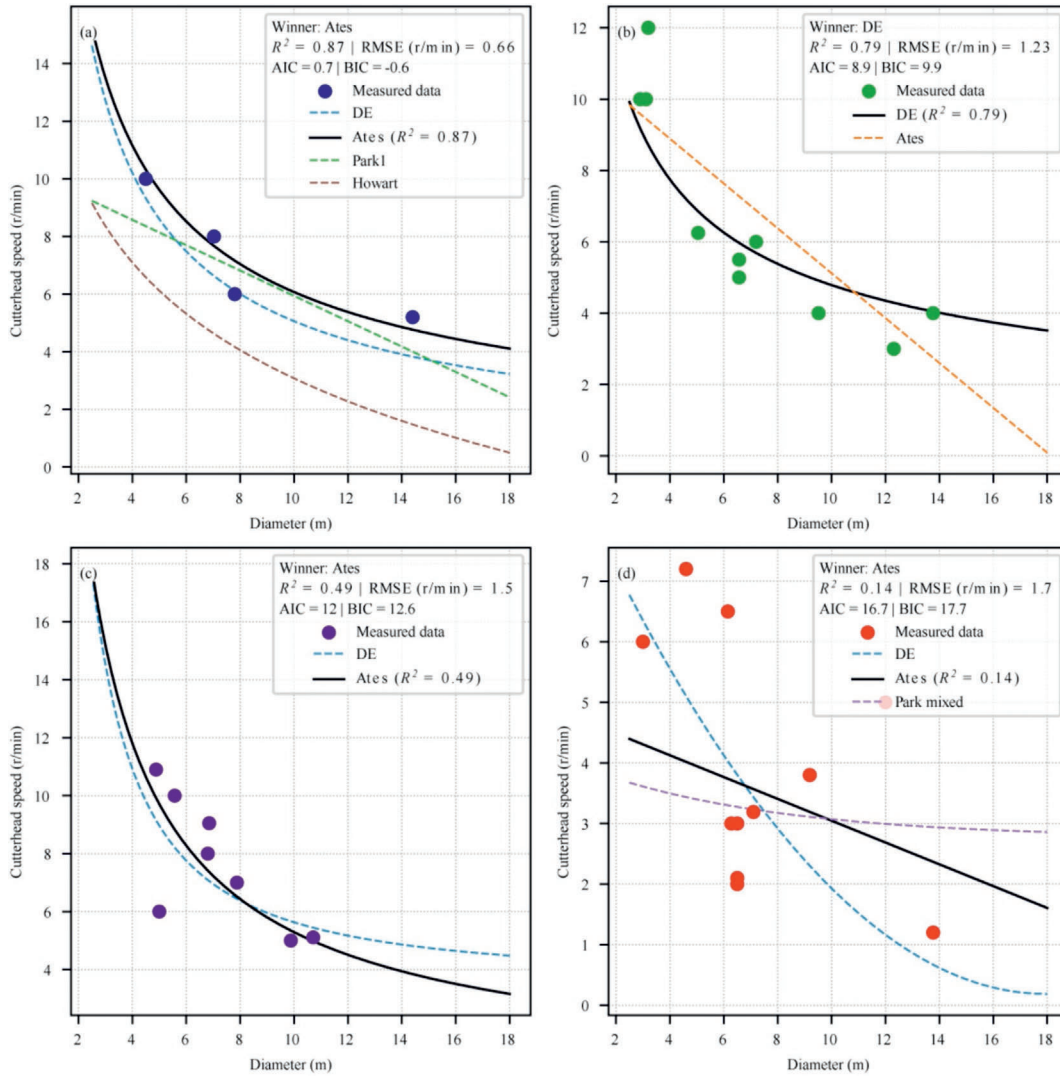


Fig. 10. Cutterhead speed versus diameter: comparison of model predictions and validation dataset results by TBM type. (a) Open TBMs, (b) SS TBMs, (c) DS TBMs, and (d) EPBs.

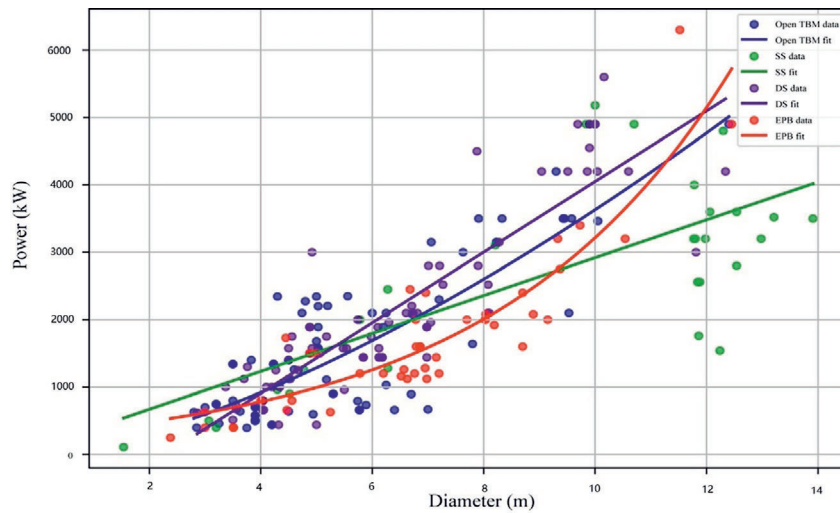


Fig. 11. Power vs. excavation diameter for all the TBM types.

Table 5
Summary of power estimation equations $P(D)$ for different TBM types under various geological conditions.

TBM type	Geology	Equation $P(D)$	R^2	Source
Open TBM	Rock	$P = 115.33D^{1.498}$	0.67	DE
SS	Fractured rock	$P = 281.10D + 108.32$	0.51	DE
DS	Fractured rock	$P = 523.94D - 1189.70$	0.79	DE
EPB	Soil/Soft ground	$P = 305.65e^{0.2353D}$	0.82	DE
EPB	Soft ground	$P = e^{(8.84 + 0.65D + 0.01D^2)}$	0.93	Park
EPB	Mixed ground	$P = e^{(5.74 + 0.20D)}$	0.86	Park
DS	Fractured rock	$P = 613.59D - 1824.44$	0.60	Park
Open TBM	Rock	$P = 350.60D + 169.62$	0.61	Park

more slowly and irregularly. EPBs follow a much steeper curve, approximately proportional to $D^{2.5}$, especially at large diameters, highlighting how machine design and geology influence real power demands. Table 5 summarizes the power–diameter equations by TBM type, including geology, model form, R^2 , and source for each case.

The validation dataset was used to check the absolute and relative accuracy of all power–diameter equations

listed in Table 5. Figure 12 compares the predicted torque values with actual measurements for each TBM type, showing how well each model fits real-world data across different machines.

The Park model best fits Open TBM data (Fig. 12(a)), explaining 62% of the power variation ($R^2 = 0.62$). Its lower AIC (29) and BIC (26.4) values compared with those of DE model indicate a more efficient fit. The RMSE is

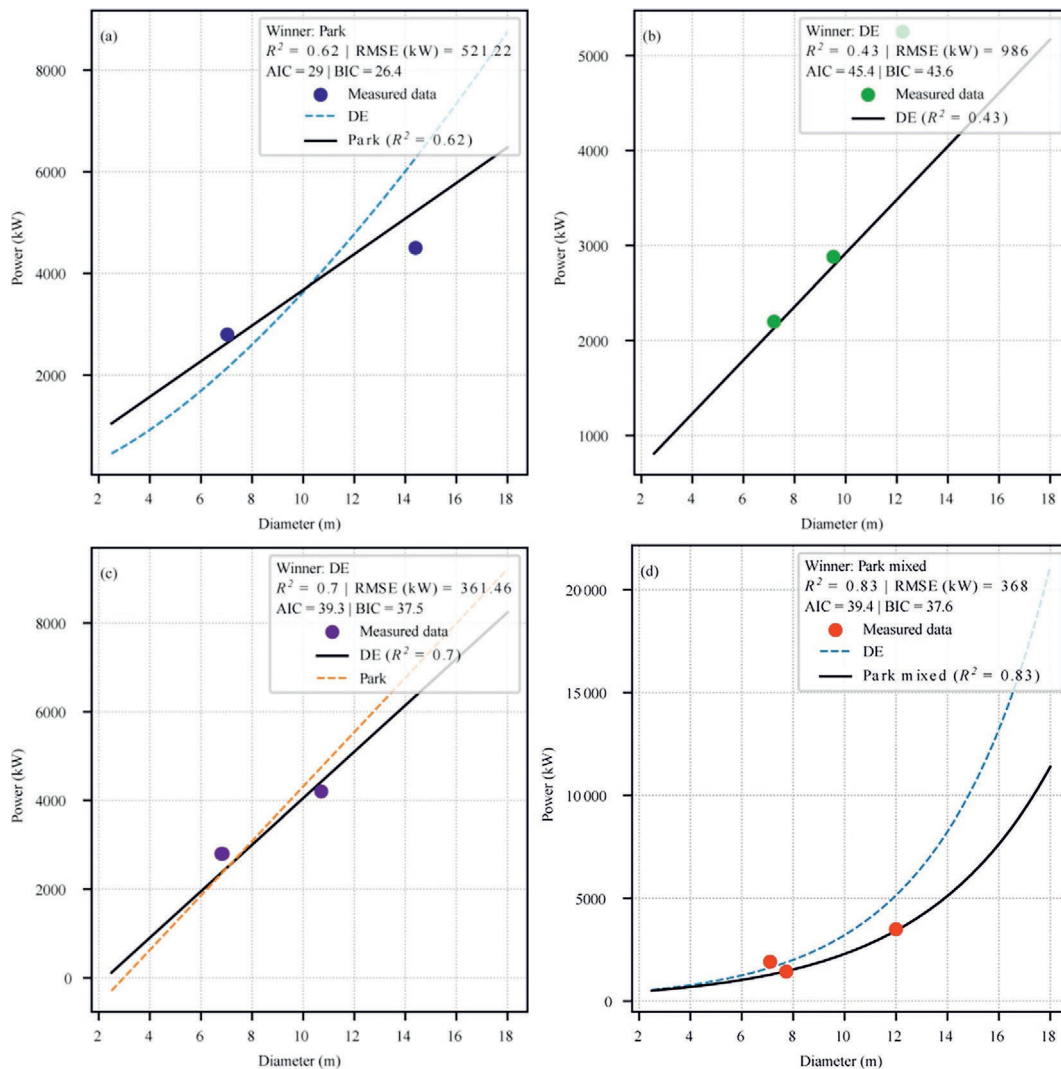


Fig. 12. Power versus diameter: comparison of model predictions and validation dataset results by TBM type. (a) Open TBMs, (b) SS TBMs, (c) DS TBMs, and (d) EPBs.

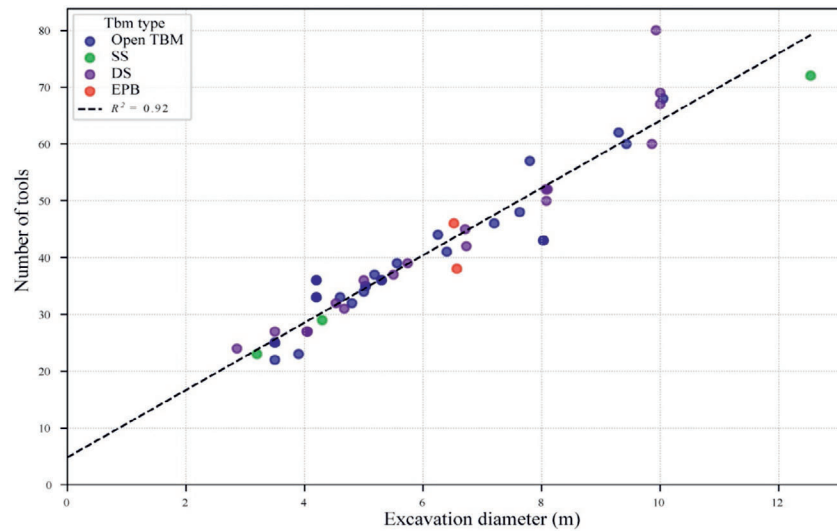


Fig. 13. Number of tools vs. excavation diameter for all TBM types.

521.22 kW (9.9%), which decreases to 442 kW (8.4%) under cross-validation, confirming both accuracy and stability.

For the single-shield (SS) data (Fig. 12(b)), the DE model performs best despite moderate predictive accuracy. It achieves $R^2 = 0.43$, reflecting the variability associated with different ground conditions. It also has the lowest AIC (45.4) and BIC (43.6) among the SS models. The RMSE is 986 kW (18.8%), reduced to 622 kW (11.9%) during cross-validation, indicating improved generalization.

The DE model also performs best for the DS data (Fig. 12(c)), with $R^2 = 0.70$. It has lower AIC (39.3) and BIC (37.5) values than the Park model, indicating a better balance between accuracy and efficiency. The RMSE is 361.46 kW (6.9%), dropping to 350 kW (6.7%) in cross-validation, confirming model stability.

For the EPB data (Fig. 12(d)), the Park-Mixed model provides the best performance. It explains 83% of power variation ($R^2 = 0.83$) and has lower AIC (39.4) and BIC (37.6) values than the DE model. The RMSE is 368 kW (7.0%), improving to 241 kW (4.6%) under cross-validation, demonstrating excellent generalizability.

4 Tools

As TBM diameter increases, the cutterhead's surface area expands, requiring more cutters to fully cover the tunnel face. Park et al. (2025) and Rostami (1997) observed a consistent trend: cutter count increases steadily with diameter across a wide range of projects. Although the exact formulations differ, the underlying principle remains the same: larger TBMs require more cutters because they engage a larger tunnel face.

Manufacturers typically follow established design guidelines, especially for hard rock TBMs, where a fixed number of disc cutters is installed per diameter unit. For instance, medium-size machines may use 40–50 cutters, whereas larger machines may require up to 70 cutters (Rostami &

Chang, 2017). This standard accounts for cutterhead layout, cutter spacing, and thrust distribution. Figure 13 shows a strong correlation between excavation diameter and the number of tools based on this study's data.

The plot reveals a strong linear relationship between TBM diameter and cutterhead tool count across all major machine types (Open, SS, DS, and EPB) supporting standard practice: tool numbers increase proportionally with tunnel diameter. Hard rock TBMs (Open, SS, DS) show similar tool counts at equivalent diameters, though DS machines typically use slightly more, and SS the fewest. EPBs generally require fewer disc cutters than rock TBMs. While the trend is meaningful, a larger dataset is needed for robust prediction.

Tool density refers to the number of cutting tools (disc cutters, scrapers, etc.) per square meter of cutterhead face area. Figure 14 shows its inverse relationship with excavation area: as the diameter increases, each tool covers a larger surface, reducing tool density. Consequently, larger TBMs offer more efficient tool spacing and improved economies of scale.

Geology directly influences tool density. In hard rock with high UCS, more cutters or tighter spacing is required, resulting in higher tool density. In fractured rock, spacing can be widened, lowering density. Abrasive soft ground causes greater tool wear, requiring closer spacing and slightly higher density. In mixed ground, TBMs often use both disc cutters and scrapers, increasing the tool count and overall density to maintain cutting efficiency and tool life.

Figure 15 compares tool density distributions across TBM types via minimum, mean, and maximum values. Rock TBMs (especially DSs and SSs) show wide variations in tool density, reflecting adaptations to heterogeneous rock conditions. DS and SS machines exhibit the highest maximum tool density and are suitable for intensive cutting in complex geology. Their average tool densities are also consistently higher than those of other TBM types.

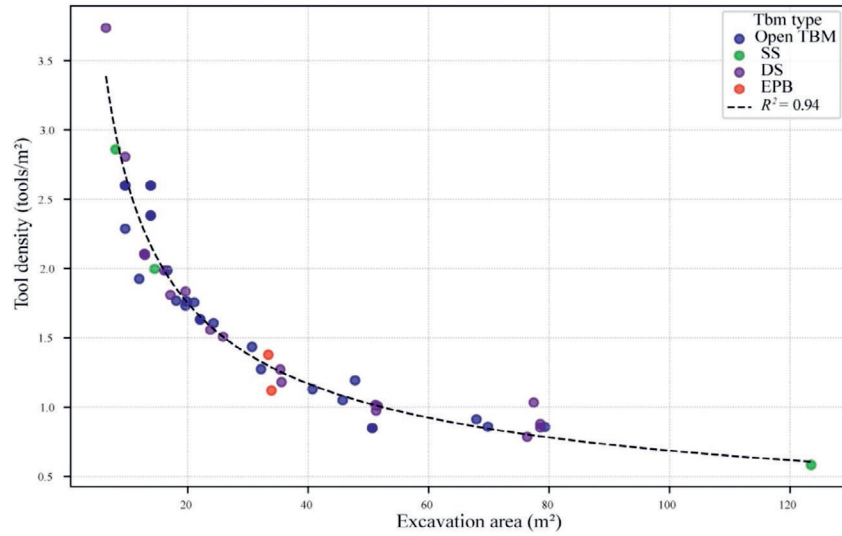


Fig. 14. Tool density vs. excavation area.

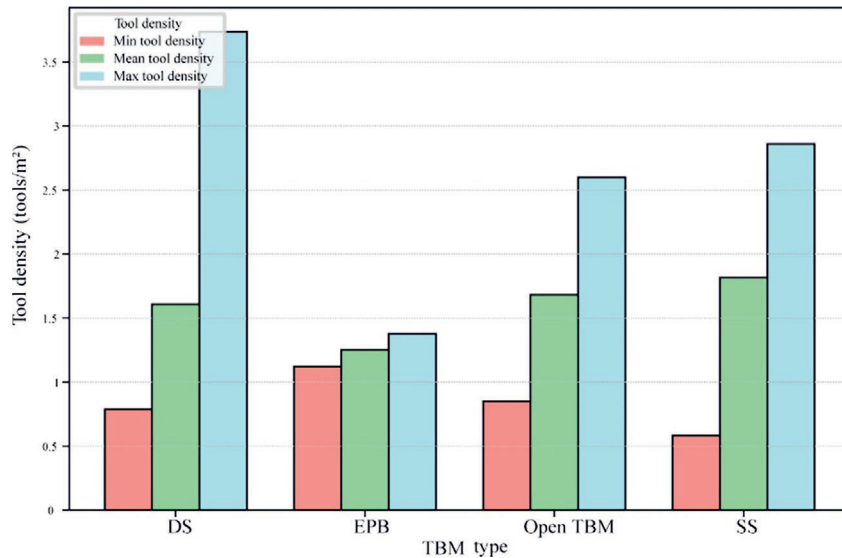


Fig. 15. Tool density used in different types of TBMs.

EPB and Open TBMs exhibit lower average and maximum tool densities. EPBs have the lowest, reflecting their efficiency in soft ground, where fewer tools suffice to manage pressure and muck flow. These results suggest that such TBMs are optimized for uniform, less abrasive soils with minimal tool-ground interaction.

The validation dataset lacked sufficient entries to fully confirm the accuracy of the equations in Table 6, preventing complete model validation. All equations from this study

(DE) and previous work (Ates) are listed to enhance transparency and enable future evaluation. Using all available tool data, the DE equation produced yielded a strong general correlation with an R^2 of = 0.92 across all TBM types.

5 Results

To objectively assess the best-performing models for each TBM type and parameter, a simple scoring system

Table 6
Summary of the number of tool estimation equations $N_T(D)$ for different TBM types under various geological conditions.

TBM type	Geology	Equation $N_T(D)$	R^2	Source
All TBMs		$N_T = 5.9288D + 4.8282$	0.92	DE
Open TBM	Rock	$N_T = 5.5221D + 7.9216$	0.95	Ates
SS TBM	Fractured rock	$N_T = 5.6216D + 4.9722$	0.95	Ates
DS TBM	Fractured rock	$N_T = 6.0679D + 5.3588$	0.95	Ates

called the “fit score” was developed. Based on the absolute evaluation of previously identified top models, it considers key metrics including R^2 , RMSE, RMSE (%), AIC, BIC, CV RMSE, and CV RMSE (%). The Fit Score reflects each model’s predictive strength and reliability, enabling quick comparisons across TBM types and variables without reanalyzing raw data. The scoring criteria are shown in Table 7, and the results with model assessments are listed in Table 8.

To supplement Table 8, the heatmap in Fig. 16 provides a quick visual summary of score distribution. Each cell displays the fit score of the top-performing model for each TBM type and performance parameter (thrust, torque, power, RPM). The color scale ranges from blue (low) to

red (high), highlighting strong or weak model performance at a glance.

To fully assess the robustness of each winning equation in Table 8, an additional layer was added by analyzing the confidence levels of the datasets. The aim was to evaluate how reliably each dataset supported its corresponding model. For every TBM type, the number of data points used to form power–diameter, torque–diameter, thrust–diameter, and RPM–diameter pairs was counted. These counts generated “confidence level heatmaps” that visually represent the reliability of the data supporting each TBM performance relationship. These heatmaps are shown in Fig. 17.

Table 7
Fit score scale.

Fit score	Interpretation	Statistical criteria
5	Outstanding fit	$R^2 > 0.80$ and $RMSE < 8\%$
4	Very good fit	R^2 between 0.65 and 0.80 and $RMSE$ between 8% and 12%
3	Good fit	R^2 between 0.45 and 0.65 and $RMSE$ between 10% and 18%
2	Moderate fit	R^2 between 0.30 and 0.45 and/or $RMSE$ between 15% and 20%
1	Weak fit	R^2 between 0.15 and 0.30 and $RMSE > 15\%$
0	Very weak/No useful prediction	$R^2 < 0.15$

Table 8
Summary of the best-fitting models for each TBM type.

Model name	Why it wins	Fit quality	Fit score (0–5)
OpenTBM-Thrust-DE	<ul style="list-style-type: none"> $R^2 = 0.55$ $RMSE = 2.22$ 	Good model explaining over half of the thrust variance with low error.	3
SS-Thrust-Ates	<ul style="list-style-type: none"> $R^2 = 0.42$ $RMSE = 11.9\%$ 	Acceptable, moderate scatter in predictions.	2
DS-Thrust-DE-SoftGround	<ul style="list-style-type: none"> $R^2 = 0.68$ $RMSE = 7.61\%$ 	Strong, captures two-thirds of the variance with low error.	4
EPB-Thrust-Ates	<ul style="list-style-type: none"> $R^2 = 0.79$ $RMSE = 10.45$ 	Very good, nearly 80% variance explained with moderate errors.	4
OpenTBM-Torque-Park	<ul style="list-style-type: none"> $R^2 = 0.73$ $RMSE = 9.28\%$ 	Solid captures most variation with an acceptable prediction error.	4
SS-Torque-DE	<ul style="list-style-type: none"> $R^2 = 0.59$ $RMSE = 16.57\%$ 	Fair, noticeable scatter, but better than alternatives.	3
DS-Torque-Park	<ul style="list-style-type: none"> $R^2 = 0.67$ $RMSE = 14.21\%$ 	Fairly good, acceptable balance between fitness and simplicity.	3
EPB-Torque-DE	<ul style="list-style-type: none"> $R^2 = 0.89$ $RMSE = 8.56\%$ 	Outstanding, very high fit quality and consistency.	5
OpenTBM-RPM-Ates	<ul style="list-style-type: none"> $R^2 = 0.87$ $RMSE = 5.50\%$ 	Excellent, ~90% variance explained and low error.	5
SS-RPM-DE	<ul style="list-style-type: none"> $R^2 = 0.79$ $RMSE = 10.24\%$ 	Very good, strong generalization and reasonable errors.	4
DS-RPM-Ates	<ul style="list-style-type: none"> $R^2 = 0.49$ $RMSE = 12.46\%$ 	Acceptable, captures about half the variance, and has moderate errors.	3
EPB-RPM-Ates	<ul style="list-style-type: none"> $R^2 = 0.14$ $RMSE = 14.14$ 	Weak, poor variance capture and high errors.	1
OpenTBM-Power-Park	<ul style="list-style-type: none"> $R^2 = 0.62$ $RMSE = 9.93\%$ 	Good capture of power variation, reasonable prediction accuracy.	3
SS-Power-DE	<ul style="list-style-type: none"> $R^2 = 0.43$ $RMSE = 18.78\%$ 	Moderate, predicts fairly but not highly precisely.	2
DS-Power-DE	<ul style="list-style-type: none"> $R^2 = 0.70$ $RMSE = 6.89\%$ 	Very good, strong fit with low error and good stability.	4
EPB-Power-ParkMixed	<ul style="list-style-type: none"> $R^2 = 0.83$ $RMSE = 7.01\%$ 	Excellent, it explains the majority of the variation with low error.	5

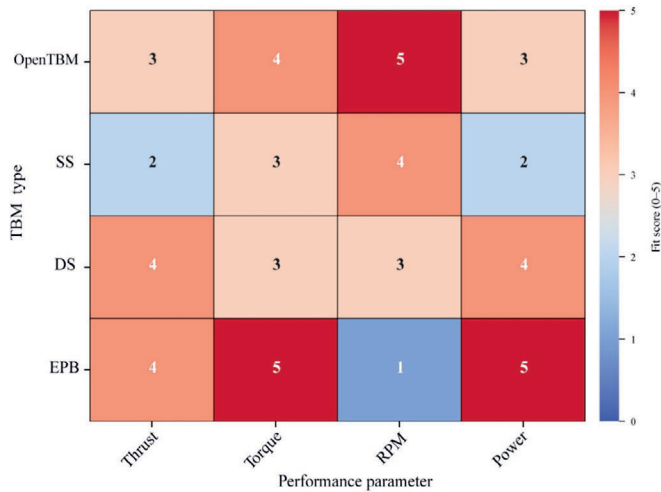


Fig. 16. Heatmap of winning model scores by TBM type and parameter.

The heatmaps present confidence levels for thrust, torque, power, and RPM across TBM types (Open, SS, DS, EPB) and data sources (Park, Ates, and this study). Here, confidence reflects the reliability of the data based on the sample size. A custom scale classifies values into six categories: >100 (level 5, highest), 75–100 (level 4), 50–74 (level 3), 25–49 (level 2), 10–24 (level 1), and <10 (level 0, very low). Original counts were mapped to these categories; missing values were treated as zero. A “cool-warm” color scale—from blue (low) to red (high)—helps visualize the strength of each dataset.

To complement the Fit Scores and Confidence Level Heatmaps, a final tool, the Reliability Matrix, was developed. This matrix integrates model fit and data confidence into a single color-coded table. The horizontal axis represents confidence scores, indicating the amount of real TBM data used for validation. In contrast, the vertical axis shows fit scores, reflecting model accuracy as measured by

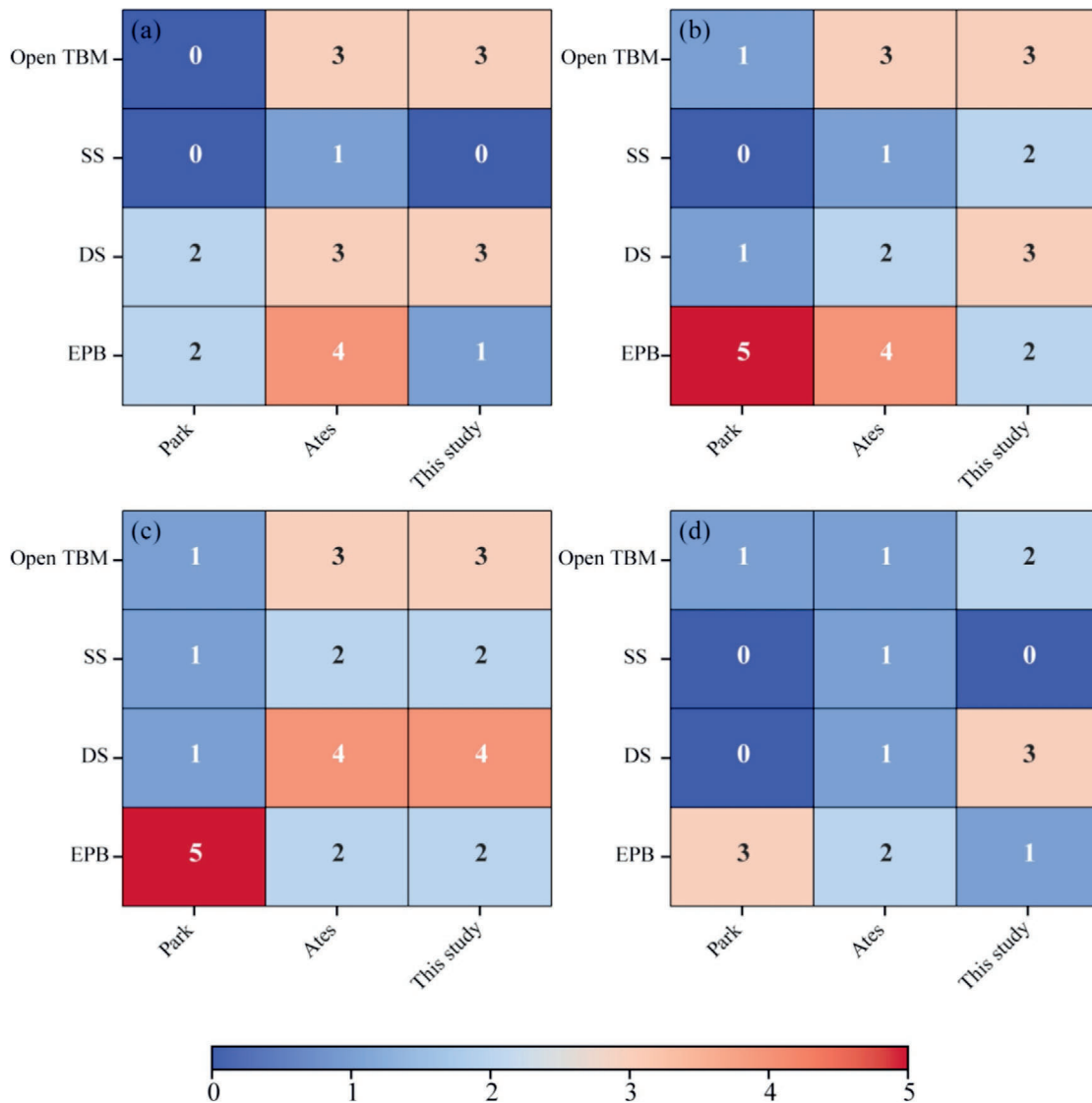


Fig. 17. Confidence level heatmaps for TBM performance parameters across different TBM types and data sources. (a) Thrust–diameter confidence level, (b) torque–diameter confidence level, (c) power–diameter confidence level, and (d) RPM–diameter confidence level.

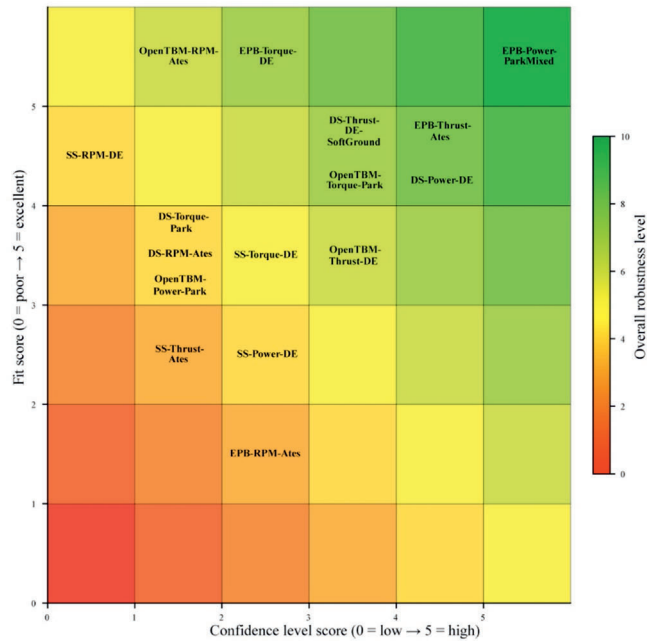


Fig. 18. Reliability matrix combining equation fit (vertical axis) and dataset confidence (horizontal axis).

R^2 , RMSE, and information criteria. Each TBM type and performance parameter is positioned at the intersection of its respective fit and confidence scores. When models tie, their names are stacked. The matrix is illustrated in Fig. 18.

Background colors provide instant visual cues about model robustness: deep green (upper-right) marks accurate equations supported by abundant data—ideal for design or forecasting. Yellow indicates moderate fits or datasets that warrant local verification. Red–orange (lower-left) highlights models with poor fit or weak data; in such cases, more data or a new formulation is recommended.

6 Discussion

Geology is the primary factor in selecting a TBM type (open, single-shield, double-shield, EPB, slurry, or multi-mode), since ground conditions directly affect cutterhead design, shield configuration, ground conditioning, and tool wear. Properties such as uniaxial compressive strength, abrasivity, fracturing, groundwater pressure, etc., often decide whether a project succeeds or fails. Likewise, the tunnel's intended use (whether for infrastructure, road traffic, hydropower, or other purposes) determines the allowable excavation diameter, although design adjustments may accommodate specific constraints. While geology is the dominant driver of TBM behavior, excavation diameter also strongly influences thrust, torque, power, and wear. Understanding TBM performance, therefore, requires evaluating not only geology but also its interaction with diameter.

Modeling this link is challenging. Geological properties can vary significantly along with the exact alignment, and

even detailed site investigations cannot fully capture this variability. At the same time, isolating the effect of diameter is extremely difficult. A clear test would require two identical TBMs from the same manufacturer, operating in the same geology, depth, and overburden but with different cutterhead sizes (for example, one with a 5 m head and another with a 10 m head), placed far enough apart to avoid stress interference. In practice, such conditions are almost impossible to achieve, leaving most models partial and unable to separate geology from diameter fully.

Although isolating the diameter perfectly is not feasible, empirical diameter-based models remain valuable. They provide structured benchmarks that highlight typical ranges for thrust, torque, power, and other performance indicators. This helps engineers identify deviations that may signal geological complications or operational issues. However, the usefulness of such models depends heavily on data quality and scope. Past studies have faced significant limitations: narrow diameter ranges, exclusion of large machines, underrepresentation of installed power, small or outdated datasets, and a lack of independent validation or structured reliability checks. These shortcomings reduce real-world applicability and leave engineers uncertain about how much confidence they can place in simple 1D diameter-based models.

This study responds directly to these gaps. A much broader dataset covering all major TBM types was compiled, and correlations were tested between diameter and thrust, torque, power, RPM, and tool count. Multiple functional forms were evaluated, the best-fit equations were selected, and results were benchmarked against existing models. A separate validation dataset was used to test predictive strength, and a reliability matrix was introduced to compare model robustness across TBM categories. By doing so, the study clarifies not only how diameter affects TBM performance but also how reliable these models are, and under which conditions they can be trusted.

The findings show strong correlations between diameter and key performance metrics, but also confirm that these models have limitations. They rely on project-wide averages that may hide local extremes, and their reliability decreases for very large-diameter TBMs (>10 m) where data remain scarce. Uncertainties remain because part of the dataset comes from published and online sources that cannot always be fully verified. While all models were assessed consistently using R^2 , AIC, BIC, and RMSE, equal testing does not imply equal reliability. For this reason, diameter-based models should not be used alone, but rather integrated with geotechnical investigations and numerical simulations.

Even with these limits, the models have clear practical value. They allow project teams to check whether TBM performance aligns with expectations and to take corrective action if deviations occur. Their simplicity makes them especially useful in feasibility and preliminary design phases, where quick checks and early decisions are required. They also support real-time monitoring during

excavation and provide rapid guidance for auxiliary or rescue tunnels, where fast data-driven judgments are needed in the same geological context.

7 Conclusions

A detailed analysis of cutter diameter effects on TBM performance, covering torque, thrust, power, cutter-head speed, and tool count, revealed apparent, nonlinear shifts across all parameters as diameter changes. Because these effects vary by machine type, geological variability was addressed indirectly by examining four TBM types designed for different ground conditions. Statistical models were then applied to quantify diameter effects, and the findings were validated using two additional modeling approaches and an independent dataset.

The study both confirmed and refined several known trends: for double shield TBMs, thrust followed a soft ground model ($R^2 = 0.68$), while EPB machines exhibited an exponential thrust relationship ($R^2 = 0.79$). Torque scaled approximately with the cube of diameter, with a quadratic model providing the best fit for open TBMs ($R^2 = 0.73$) and an even stronger fit for EPBs ($R^2 = 0.89$). Cutterhead speed decreased with increasing diameter, matching an inverse power-law form in open TBMs ($R^2 = 0.87$) and showing a clear inverse trend in single shield machines ($R^2 = 0.79$). However, EPBs displayed greater variability ($R^2 = 0.14$). Power requirements increased faster than linearly, fitting an exponential curve for EPBs ($R^2 = 0.83$) and a linear plus form for double-shield machines ($R^2 = 0.70$). Tool count increased in a simple linear manner, following $N = 5.93D + 4.83$ ($R^2 = 0.92$).

To address limitations in data quality and sample size across this study, previous research by Park and Ates, and the validation dataset, a reliability matrix was introduced. This matrix plots model fit against data confidence, distinguishing highly accurate but sparsely supported models (e.g., EPB Torque, DE model: Fit = 5, Conf = 1) from less precise but well-supported ones (e.g., SS Thrust Ates model: Fit = 2, Conf = 5). This two-axis framework highlights the equations that are statistically reliable and practically applicable.

Data availability

The data that support the findings of this study are available from the corresponding author upon reasonable request.

CRedit authorship contribution statement

Oveis Farzay: Writing – original draft, Visualization, Validation, Methodology, Investigation, Data curation, Conceptualization. **Marilena Cardu:** Writing – review & editing, Supervision, Conceptualization.

Declaration of competing interest

The authors declare that they have no known competing financial interests or personal relationships that could have appeared to influence the work reported in this paper.

Acknowledgement

We acknowledge the contributions of industry sources including Robbins, Herrenknecht AG, and CREG Company.

References

- Ates, U., Bilgin, N., & Copur, H. (2014). Estimating torque, thrust and other design parameters of different type TBMs with some criticism to TBMs used in Turkish tunneling projects. *Tunnelling and Underground Space Technology*, 40, 46–63.
- Ban, C., Gong, Q., Zhou, X., & Li, S. (2020). Analysis of TBM disc cutter wear: A case study of a water conveyance tunnel project in Xinjiang, China. *IOP Conference Series: Earth and Environmental Science*, 570(5), 052026.
- Barla, G., & Pelizza, S. (2000). TBM tunnelling in difficult ground conditions. In *Proceedings of the ISRM International Symposium, Melbourne, Australia, November 2000* (Paper No. ISRM-IS-2000-037). International Society for Rock Mechanics and Rock Engineering (ISRM).
- Barton, N. (1999). TBM performance estimation in rock using QTBM. *Tunnels and Tunnelling International*, 31(9), 30–34.
- Bbt, S. E. (2025). *Brenner Base Tunnel Project Overview*. <https://www.bbt-se.com/en/tunnel/project-overview/>.
- Bilgin, N., & Acun, S. (2021). The effect of rock weathering and transition zones on the performance of an EPB-TBM in complex geology near Istanbul, Turkey. *Bulletin of Engineering Geology and the Environment*, 80(4), 3041–3052.
- Bilgin, N., & Algan, M. (2012). The performance of a TBM in a squeezing ground at Uluabat, Turkey. *Tunnelling and Underground Space Technology*, 32, 58–65.
- Bilgin, N., Balci, C., Acaroglu, O., Tunçdemir, H., Eskikaya, S., Akgul, M., & Algan, M. (1999). The performance prediction of a TBM in Tuzla–Dragos sewerage tunnel. In *Proceedings of the World Tunnel Congress' 99, Oslo, Norway, 31 May–3 June 1999* (pp. 817–822).
- Bilgin, N., Copur, H., & Balci, C. (2012). Effect of replacing disc cutters with chisel tools on performance of a TBM in difficult ground conditions. *Tunnelling and Underground Space Technology*, 27(1), 41–51.
- Brenner Basistunnel, B. S. (2025). *Project overview*. <https://www.bbt-se.com/en/tunnel/project-overview/>.
- Bruland, A. (1998). Hard rock tunnel boring. [Ph. D. Thesis, Norwegian University of Science and Technology, Trondheim, Norway].
- Cardu, M., Catanzaro, E., Farinetti, A., Martinelli, D., & Todaro, C. (2021). Performance analysis of tunnel boring machines for rock excavation. *Applied Sciences*, 11(6), 2794.
- Cardu, M., Di Giovanni, A., Saltarin, S., & Todaro, C. (2023a). An analysis of metal wear in rock excavation by TBM. Expanding underground - knowledge and passion to make a positive impact on the world. In *Proceedings of the ITA-AITES World Tunnel Congress* (pp. 1183–1192).
- Cardu, M., Farzay, O., Shakouri, A., Jamali, S., & Jamali, S. (2023b). Feasibility assessment of acid gas injection in an Iranian offshore aquifer. *Applied Sciences-Basel*, 13(19), 10776.
- Cardu, M., Todaro, C., Farzay, O., Di Giovanni, A., & Saltarin, S. (2024). Performance analysis of TBM excavation parameters related to small-diameter horizontal and inclined tunnels. In *Tunnelling for a Better Life* (pp. 1669–1674). Taylor & Francis.
- Caulfield, R., Kieffer, D. S., Tsztoo, D. F., & Cain, B. (2005). Seismic design measures for the retrofit of the claremont tunnel. *RETC Proceedings California*, 1128–1138.

- Chang, S.-H., Choi, S.-W., Bae, G.-J., & Jeon, S. (2006). Performance prediction of TBM disc cutting on granitic rock by the linear cutting test. *Tunnelling and Underground Space Technology*, 21(3/4), 271.
- Chapuis, A., & Yiu, D. (2006). De Tuen Mun à Tsz Wan Shan: les tribulations d'un tunnelier français au service de China Light & Power Hong Kong: Réseaux-Galeries Multiréseaux. *Travaux (Paris)*, (835), 37–41.
- Cho, J.-W., Jeon, S., Jeong, H.-Y., & Chang, S.-H. (2013). Evaluation of cutting efficiency during TBM disc cutter excavation within a Korean granitic rock using linear-cutting-machine testing and photogrammetric measurement. *Tunnelling and Underground Space Technology*, 35, 37–54.
- Co, S. I. (2025, 2025/04/15). *Southern Extension of Tehran Metro Line 6*. <https://sabit-intl.com/en/projects>.
- Farrokh, E., Rostami, J., & Laughton, C. (2012). Study of various models for estimation of penetration rate of hard rock TBMs. *Tunnelling and Underground Space Technology*, 30, 110–123.
- Farzay, O., Cardul, M., & Jamali, S. (2025). Sensitivity and monte carlo analysis of open TBM diameter: Impacts on power, thrust, and torque. *Geotechnical and Geological Engineering*, 43(6), 240.
- Farzay, O., Khatibi, S., Aghajanzadeh, A., Shakhouri, A., & Al-Ajmi, A. M. (2022a). A numerical method for potential implementation of underbalanced drilling in high pore pressure reservoirs. *International Journal of Oil, Gas and Coal Technology*, 30(3), 283–299.
- Farzay, O., Shakhouri, A., Gholami, R., & Al-Ajmi, A. M. (2022b). Optimum directional well path design considering collapse and fracture pressures. *International Journal of Oil, Gas and Coal Technology*, 30(4), 388–414.
- Garshol, K. F., Melbye, T. A., & Woldmo, O. (2000). Ground Water Control and Rock Support in TBM-Tunnelling in Hong Kong. In *IABSE Congress Report (Vol. 16, No. 15, pp. 823–830)*. International Association for Bridge and Structural Engineering.
- Graham, P. (1976). Rock exploration for machine manufacturers. In *Proceedings of Symposium on Exploration for Rock Engineering* (pp. 173–180).
- Grima, M. A., & Babuška, R. (1999). Fuzzy model for the prediction of unconfined compressive strength of rock samples. *International Journal of Rock Mechanics and Mining Sciences*, 36(3), 339–349.
- Hassanpour, J., Rostami, J., & Zhao, J. (2011). A new hard rock TBM performance prediction model for project planning. *Tunnelling and Underground Space Technology*, 26(5), 595–603.
- Hassanpour, J., Rostami, J., Zhao, J., & Azali, S. T. (2015). TBM performance and disc cutter wear prediction based on ten years experience of TBM tunnelling in Iran. *Geomechanics and Tunneling*, 8(3), 239–247.
- Herrenknecht, A. G. (2024). Herrenknecht returns to the Gotthard. <https://www.herrenknecht.com/en/newsroom/pressreleasedetail/herrenknecht-kehrt-an-den-gotthard-zurueck/>.
- Herrenknecht, A. G. (2025a, 2025/04/15). *Barcelona Metro Line 9*. <https://www.herrenknecht.com/en/references/referencesdetail/barcelona-metro-line-9/>.
- Herrenknecht, A. G. (2025b, 2025/04/15). *Gotthard Base Tunnel*. <https://www.herrenknecht.com/en/references/referencesdetail/gotthard-base-tunnel/>.
- Herrenknecht, A. G. (2025c, 2025/04/15). *Istanbul Metro*. <https://www.herrenknecht.com/en/references/referencesdetail/istanbul-metro/>.
- Howart, D. F. (1994). Database of TBM projects undertaken between 1950 and 1990 and an assessment of associated ground-strength limitations. *Tunnelling and Underground Space Technology*, 9(2), 209–213.
- Implenia, A. G. (2023, 2023/05/08). *Second tube Gotthard Tunnel: first tunnel boring machine "Carla" at target*. <https://www.implenia.com/en/media/news-article/tbm-carla/>.
- Jodehl, A., Berns, J., Thewes, M., & König, M. (2025). Improving the performance prediction of process simulation models for TBM tunneling using real-time project data. *Applied Sciences*, 15(4), 1969.
- Keiper, K., Crapp, R., & Amberg, F. (2010). Assessment of the interaction of TBM and rock mass in rock tunnelling based on geomechanical calculations. *Geomechanics and Tunneling*, 3(5), 534–546.
- Khatibi, S., Aghajanzadeh, A., Ostadhassan, M., & Farzay, O. (2018a). Evaluating single-parameter parabolic failure criterion in wellbore stability analysis. *Journal of Natural Gas Science and Engineering*, 50, 166–180.
- Khatibi, S., Farzay, O., & Aghajanzadeh, A. (2018b). A Method to Find Optimum Mud Weight in Zones With No Safe Mud Weight Windows. *ARMA US Rock Mechanics/Geomechanics Symposium* (pp. ARMA-2018). ARMA.
- Khatibi, S., Ostadhassan, M., Farzay, O., & Aghajanzadeh, A. (2019). Seismic driven geomechanical studies: A case study in an offshore gas field. *53rd U.S. Rock Mechanics/Geomechanics Symposium*.
- King, M., Thomas, I., & Stenning, A. (2017). Crossrail project: machine-driven tunnels on the Elizabeth line, London. *Proceedings of the Institution of Civil Engineers-Civil Engineering*, 170(5), 31–38.
- Krause, T. (1987). *Shield Tunneling with Hydraulic and Soil-Supported Tunnel Face* [Doctoral dissertation, Technical University of Braunschweig] (in German).
- Laughton, C. (1998). *Evaluation and prediction of tunnel boring machine performance in variable rock masses* [Doctoral dissertation, The University of Texas at Austin].
- Lu, C., Liu, C., & Zhang, X. (2023). Segment thickness design and bearing performance analysis of large inner-diameter shield tunnel under lateral unloading. *Applied Sciences*, 13(21), 11871.
- Machida, A., & Uomoto, T. (1997). Recommendation for design and construction of concrete structures using continuous fiber reinforcing materials. Tokyo, Japan: Japan Society of Civil Engineers.
- Macias, F. J. (2016). Hard rock tunnel boring: performance predictions and cutter life assessments [Doctoral dissertation, NTNU].
- Merguerian, C. (2010). Techniques of TBM tunnel mapping-the Queens Tunnel, NYC.
- Moon, T., & Oh, J. (2012). A study of optimal rock-cutting conditions for hard rock TBM using the discrete element method. *Rock Mechanics and Rock Engineering*, 45(5), 837–849.
- Mostafa, S., & Sousa, R. L. (2024). Enhancing ground classification models for TBM tunneling: Detecting label errors in datasets. *Computers and Geotechnics*, 170, 106301.
- Okano, N., Watabe, Y., Kokubo, H., & Takagi, K. (2000). Railway Tunnels Excavated by TBM and Deep Bore Blasting Method in Japan. In *IABSE Congress Report (Vol. 16, No. 15, pp. 808–815)*. International Association for Bridge and Structural Engineering.
- Ozdemir, L. (1977). *Development of theoretical equations for predicting tunnel borability* (Publication No. T-1969) [Doctoral dissertation, Colorado School of Mines].
- Pandey, P., Raina, A., Deshmukh, S., Trivedi, R., Vajre, R., & Murthy, V. (2020). Influence of geology on tunnel boring machine performance: A review. *Journal of Mining and Metallurgy*, 56(1), 1–14.
- Park, B., Lee, C., Choi, S., Kang, T., & Chang, S. (2018). Statistical analysis of TBM database to estimate technical specifications of TBMs. *Proceedings of the 2018 World Congress on Advances in Civil, Environmental, & Materials Research (ACEM18), Songdo Convensia*.
- Park, M., Ju, M., Kim, J., & Jeong, H. (2025). Measurement of TBM disc cutter wear using eddy-current sensor in different TBM chamber conditions: Insights from laboratory tests. *Sensors (Basel)*, 25(7).
- Partov, D., Ivanov, R., & Petkov, M. (2012). Survey of the design of back anchors for tunnel boring machines (TBM), used in the excavation of metro tunnels in Sofia. *Procedia Engineering*, 40, 351–356.
- Pompeu-Santos, S. (2011). Tunnels for Large Crossings: Challenges and Innovations. In *35th Annual Symposium of IABSE/52nd Annual Symposium of IASS/6th International Conference on Space Structures: Taller, Longer, Lighter-Meeting growing demand with limited resources*, London, United Kingdom, September 2011.
- Qi, G., Zhengying, W., & Hao, M. (2016). An experimental research on the rock cutting process of the gage cutters for rock tunnel boring machine (TBM). *Tunnelling and Underground Space Technology*, 52, 182–191.
- Qian, Z., Zou, J., Pan, Q., & Dias, D. (2019). Safety factor calculations of a tunnel face reinforced with umbrella pipes: A comparison analysis. *Engineering Structures*, 199, 109639.
- Ramezanzadeh, A., Rostami, J., & Kastner, R. (2005). Influence of rock mass properties on performance of hard rock TBMs. In *Proceedings of the Rapid Excavation and Tunneling Conference* (pp. 27–29).
- Ramoni, M., & Anagnostou, G. (2010). Thrust force requirements for TBMs in squeezing ground. *Tunnelling and Underground Space Technology*, 25(4), 433–455.
- Rostami, J. (1997). Development of a force estimation model for rock fragmentation with disc cutters through theoretical modeling and physical measurement of crushed zone pressure (Vol. 38). Colorado School of Mines Golden, CO, USA.
- Rostami, J. (2016). Performance prediction of hard rock Tunnel Boring Machines (TBMs) in difficult ground. *Tunnelling and Underground Space Technology*, 57, 173–182.

- Rostami, J., & Chang, S.-H. (2017). A closer look at the design of cutterheads for hard rock tunnel-boring machines. *Engineering*, 3(6), 892–904.
- Rostami, J., Farrokh, E., Laughton, C., & Eslambolchi, S. S. (2014). Advance rate simulation for hard rock TBMs. *KSCE Journal of civil engineering*, 18, 837–852.
- Rostami, J., & Ozdemir, L. (1993). A new model for performance prediction of hard rock TBMs. In *Proceedings of the Rapid Excavation and Tunneling Conference* (pp. 793).
- Salimi, A., Faradonbeh, R. S., Monjezi, M., & Moormann, C. (2018). TBM performance estimation using a classification and regression tree (CART) technique. *Bulletin of Engineering Geology and the Environment*, 77(1), 429–440.
- Salimi, A., Rostami, J., & Moormann, C. (2019). Application of rock mass classification systems for performance estimation of rock TBMs using regression tree and artificial intelligence algorithms. *Tunnelling and Underground Space Technology*, 92, 103046.
- Samadi, H., & Hassanpour, J. (2024). EPB-TBM cutterhead torque and thrust modelling in rock tunnels through an analytical method and TSFS model. *Heliyon*, 10(11).
- Shakouri, A., Farzay, O., Masihi, M., Ghazanfari, M. H., & Al-Ajmi, A. M. (2019). An experimental investigation of dynamic elastic moduli and acoustic velocities in heterogeneous carbonate oil reservoirs. *SN Applied Sciences*, 1(9), 1023.
- Shi, H., Yang, H., Gong, G., & Wang, L. (2011). Determination of the cutterhead torque for EPB shield tunneling machine. *Automation in Construction*, 20(8), 1087–1095.
- Song, T., & Zhou, S. (2008). Study on the earth pressure distribution of excavation chamber in EPB tunneling. In *Geotechnical Aspects of Underground Construction in Soft Ground* (pp. 359–364). CRC Press.
- Song, X., Liu, J., & Guo, W. (2010). A cutter head torque forecast model based on multivariate nonlinear regression for EPB shield tunneling. *International Conference on Artificial Intelligence and Computational Intelligence*, 2010, 104–108.
- Staff, T. B. M. (2024, 2024/03/08). *Seventh TBM Handed Over for the Brenner Project*. <https://tunnelingonline.com/seventh-tbm-handed-over-for-the-brenner-project/>.
- Staff, W. (2000, 2000/03/30). *TBM Experience on the Hida Tunnel*. <https://www.tunnelsandtunnelling.com/analysis/tbm-experience-on-the-hida-tunnel/>.
- Sun, W., Shi, M., Zhang, C., Zhao, J., & Song, X. (2018). Dynamic load prediction of tunnel boring machine (TBM) based on heterogeneous in-situ data. *Automation in Construction*, 92, 23–34.
- Sutcliffe, H. (1996). Tunnel Boring Machines. In J. O. Bickel, T. R. Kuesel, & E. H. King (Eds.), *Tunnel Engineering Handbook* (pp. 203–219). US: Springer.
- The Robbins, C. (2025, 2025/04/15). *The Niagara Tunnel Project*. <https://www.robbinstbm.com/projects/niagara-tunnel-project/>.
- Thibault, M. (2024, 2024/04/17). *LA Metro completes 5-year Purple Line tunneling project*. <https://www.smartcitiesdive.com/news/la-metro-tunneling-purple-line/713437/>.
- Thomas, T. (2024, 2024/08/08). *12.3m diameter TBM readies for second Gotthard Road Tunnel*. <https://tunnellingjournal.com/12-3m-diameter-tbm-readies-for-second-gotthard-road-tunnel/>.
- Tunnel, o. (2025/02/14). *Gotthard Road Tunnel: Main drive for the second tube underway since February 2025*. <https://www.tunnel-online.info/en/artikel/gotthard-road-tunnel-main-drive-for-the-second-tube-underway-since-february-2025-4226655.html>.
- Tunneling and Underground Construction. (2023). *Unprecedented in-tunnel diameter conversion of the largest hard rock TBM in the United States*. <https://tucmagazine.org/unprecedented-in-tunnel-diameter-conversion-of-the-largest-hard-rock-tbm-in-the-united-states-2/>.
- Vardakos, S., Zlatanic, S., Wongkaew, S., & Bauer, A. (2023). *Large diameter TBM tunnels – Trends in planning and design* (1 ed.). CRC Press.
- Wang, L., Gong, G., Shi, H., & Yang, H. (2012). A new calculation model of cutterhead torque and investigation of its influencing factors. *Science China Technological Sciences*, 55(6), 1581–1588.
- Wikipedia, C. (2025, 2025/04/15). *Guadarrama Tunnel*. https://en.wikipedia.org/wiki/Guadarrama_Tunnel.
- Wilfing, L. S. F. (2016). *The Influence of Geotechnical Parameters on Penetration Prediction in TBM Tunneling in Hard Rock: Special focus on the parameter of rock toughness and discontinuity pattern in rock mass* [Ph.D. thesis, Technische Universität München]. Munich, Germany.
- Yagiz, S. (2002). *Development of rock fracture and brittleness indices to quantify the effects of rock mass features and toughness in the CSM Model basic penetration for hard rock tunneling machines*. Colorado School of Mines.
- Yagiz, S., & Ozdemir, L. (2001). Geotechnical parameters influencing the TBM performance in various rocks. program with abstract. In *44th Annual Meeting of Association of Engineering Geologists*; Technical Session.
- Zheng, Y., & He, L. (2021). TBM tunneling in extremely hard and abrasive rocks: Problems, solutions and assisting methods. *Journal of Central South University*, 28(2), 454–480.
- Yazdani-Chamzini, A., & Yakhchali, S. H. (2012). Tunnel Boring Machine (TBM) selection using fuzzy multicriteria decision making methods. *Tunnelling and Underground Space Technology*, 30, 194–204.
- Zhai, S., Song, Y., & Tian, H. (2024). Development of thrust, torque, and power estimation model, and prediction performance of earth pressure balance tunnel boring machine in mixed-face strata. *Applied Sciences*, 14(13), 5887.
- Zhang, Q., Kang, Y., Zheng, Z., & Wang, L. (2013). Inverse analysis and modeling for tunneling thrust on shield machine. *Mathematical Problems in Engineering*, 2013(1), 975703.
- Zhang, Q., Qu, C., Kang, Y., Huang, G., Cai, Z., Zhao, Y., Zhao, H., & Su, P. (2012). Identification and optimization of energy consumption by shield tunnel machines using a combined mechanical and regression analysis. *Tunnelling and Underground Space Technology*, 28, 350–354.